Report of the National Research Center for Disaster Prevention, No. 23, March 1980

556.332.6

Experiments on Rain Infiltration in Soil (3)*

——Dynamic characteristics of rain infiltration and ground water flow——

By

Masaki Tominaga**

National Research Center for Disaster Prevention, Japan

Abstract

Experiments are described which were conducted to investigate mechanisms of infiltration of rain using the large scale rainfall simulator of the National Research Center for Disaster Prevention. The experiments were designed to reveal time-varying changes of water content for several kinds of soils including sandy soils and loamy soils, in response to rainfall. For this purpose, measurement of specific resistance was developed and used. The results are as follows:

1. Velocity of downward movement of the transmission front, which is boundary section between the transmission zone and the wetting zone, increases when rainfall becomes intense, in both kinds of soils.
2. Percolation at each depth reaches equilibrium with transit of the transmission front, under a constant and continuous rainfall.
3. Ground water begins to flow out when the wetting front reaches the upper bound of capillary rise above the ground water level.
4. Permeability of percolation in the equiliblium state, which is derived from the flow-out intensity of the ground water divided by the amount of increase of water content in the soil, is similar to the one of saturated infiltration that is derived from a laboratory test. This is explained by the 'Open system-Unsaturated-Capillary-Percolation' which is a modal in which water percolates through the capillary surrounded by air being connected to the outside.
5. The specific resistance increases at all points in the soil soon after rain stops.
6. 'Ponding' around the surface of the ground, which includes not only water film on the surface but also isolation of the in/out flow of air around the surface, interferes with the smooth release of air from the soil to the open air and makes rate of infiltration small.

* The present study is a part of the 'Synthetic Study on Hydrological Balance of Ground Water' performed by the Special Fund for Promoting Multi-ministrial Research Projects under the Jurisdiction of the Science and Technology Agency for fiscal year from 1976 to 1978.

** Rainfall Laboratory, Third Research Division.

1. Preface

It is necessary to investigate mechanisms of rain infiltration in soil not only to control resources of ground water but also to trace the cause of and prevent landslide or slope failure, which are often caused by rainfall. Water supplied by rainfall infiltrates the soil usually under the condition that the void of the soil is water-unsaturated and the surface of the ground is not completely covered by water. In this condition, the air and water existing among the soil particles can change their positions readily. In addition to the characteristics mentioned above, it seems that the apparent discharge of ground water is caused not only by movement of water through the soil but also by propagation of pressure in the capillary water.

In the present paper, a series of experiments on rain infiltration in soil, performed using a rainfall simulator of the National Research Center for Disaster Prevention, are discussed to investigate the mechanisms of unsaturated infiltration caused by rainfall.

2. Purpose of experiments

Field work and laboratory experiments are both useful to investigate mechanisms of infiltration. Field work is often performed in places where ground water discharge must be controlled. Laboratory experiments are conducted under controlled conditions. In field research, it is impossible to control conditions, for example the intensity or the duration of rainfall. Phenomena which can be observed in the field are compounded results of such variables. Ground water are principally supplied by rain. Much of rainfall evaporates, part of the remains flows into river, and the rest is the main source of ground water. Generally speaking, precipitation of rainfall can be observed as a discharge of ground water after a period.

From another point of view, disasters caused by rainfall, such as slope failure, landslide and failure of river banks, mainly result from weakening of soil strength against stress. In many cases, the weakening coincides with an increase in the water content of the soil. It is often observed that slope failure occurs after a small rainfall precipitation, although it has never occured by more precipitation than that. It seems that the conditions of infiltration are different, such as the distribution of water content in the ground and the precipitation supplied before the failure. Therefore, infiltration has to be investigated under conditions which includes the effects not only of soil-water content of the ground but also of the rainfall pattern.

3. Outline of experiments

Ground models were made utilizing lysimeter at the experimental site of the National Research Center for Disaster Prevention. Sand, pumice, humus and loam were selected as experimental soils. Measurements were concentrated on the observation of infiltration of water and of ground water discharge. The experiments were performed over two years. In the first year, several parameters of soil, such as compaction

Table 1 Table of Experiments.

Month/Day	Rainfall Input	Starting Time	Coarse Sand (S1)	Fine Sand (S2)		Kanuma Pumice (K)
1977,6/ 6	30* 2	14:07	1 2 3 4	1 2 3 4 5		1 2 3 4
8	50* 2	13:48	1 2 3 4	1 2 3 4 5		1 2 3 4
13	100* 2	14:01	1 2 3 4	1 2 3 4 5		1 2 3 4
16	70* 2	15:00	1 2 4	1 2 4 5		1 2 4
					Kanto Loam (L)	
11/ 7	30* 2	13:37	1 2 3 4 5	1 2 3 4 5	1 2 3 4 5	1 2 3 4 5
10	30* 4	13:17	1 2 3 4 5	1 2 3 4 5	1 2 3 4 5	1 2 3 4 5
14	50* 2	13:45	1 2 3 4 5	1 2 3 4 5	1 2 3 4 5	1 2 3 4 5
					Uncompacted Loam (L3)	
1978,4/11	50* 6	10:18	1 2 5	1 2 5	1 2 5	1 2 5
18	100*.5	13:05	1 2 5	1 2 5	1 2 5	1 2 5
25	15* 6	10:05	1 2 3 5	1 2 3 5	1 2 3 5	1 2 3 5
5/ 2	30* 6	10:16	1 2 3 5	1 2 3 5	1 2 3 5	1 2 5
10	50* 6	10:15	1 2 3 5	1 2 3 5	1 2 3 5	1 2 3 5
15	30+70* 2	13:18	1 2 3 5	1 2 3 5	1 2 5	1 2 5
22	50*.5* 3	13:14	1 2 3 5	1 2 3 5	1 2 3 5	1 2 3 5
			Humic Loam (L1)	Compacted Loam (L2)		Stratified Loam (L4)
8/11	50* 6	10:25	1 2 5	1 2 5	1 2 5	1 2 5
18	15* 6	10:48	1 2 5	1 2 5	1 2 5	1 2 5
25	30* 6	10:41	1 2 5	1 2 5	1 2 5	1 2 5
31	50* 6	10:14	1 2 5	1 2 5	1 2 5	1 2 5
9/ 6	50* 1	13:19	1 2 5	1 2 5	1 2 5	1 2 5
12	100*.5	13:32	1 2 5	1 2 5	1 2 5	1 2 5
18	30+70* 2	13:23	1 2 3 5	1 2 3 5	1 2 3 5	1 2 3 5
25	50*.5* 3	13:10	1 2 5	1 2 3 5	1 2 3 5	1 2 3 5

Measurements
1: Specific resistance
2: Discharge of ground water
3: Neutron scattering
4: Ground water level
5: Soil-moisture potential

and difference of particle sizes, intensity and duration of rainfall were checked. The following year, experiments concerned with sandy and loamy soils were conducted. All experiments are listed in **Table 1**.

(1) Ground models

Fig. 1 and **Photo 1** show the lysimeter. Soils were placed in cubic boxes of length 2.4m and with the upper side open. Four boxes were placed side by side. The area

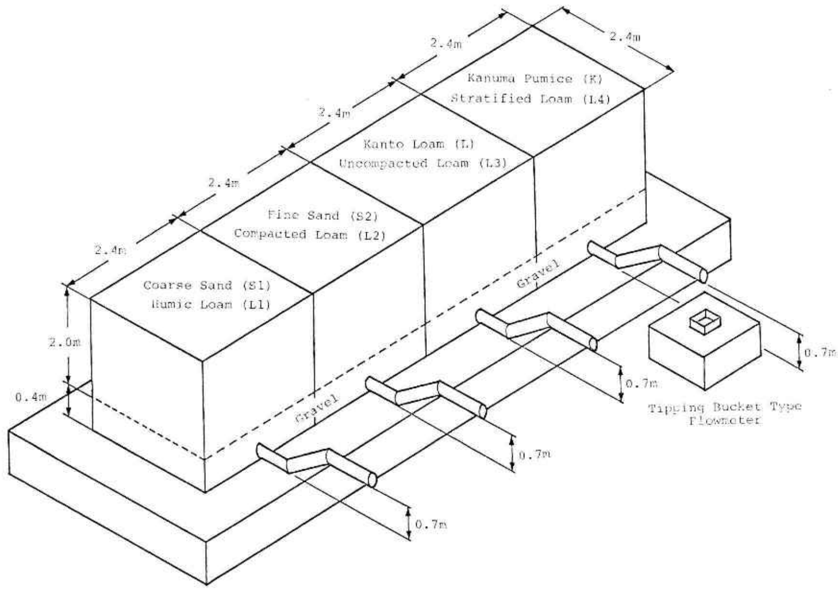

Fig. 1 Ground Models (Lysimeter).

of the upper side was as wide as possible to perform measurements which are not affected by the wall. The measurement of specific resistance can be well performed under the condition that the radius of the boxes through the sensing axis is three times wider than the interval of the electrodes (Takenaka, 1956), and the measurement of neutron scattering is affected by soil about 60cm in radius(JSSMFE, 1974). Therefore, the length of 2.4 m was used for the experimental soil boxes.

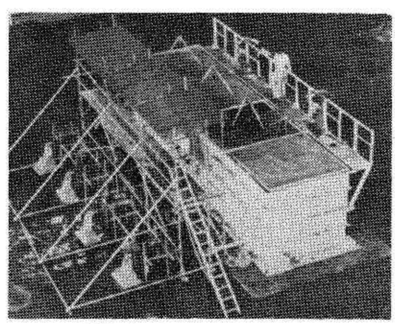

Photo 1 Lysimeter.

(2) Experimental soils

First of all, as infiltration can be classified into several types, sandy soils and a loam were chosen to illustrate fast and slow infiltration respectively. Next, loamy soils were selected as models of natural soil. All of these models were made of disturbed soils. **Table 2** shows the producing fields, compacted or not, the names of the experimental soils and the reason for selection. In **Table 3**, the particle size distributions of the experimental soils are given.

(3) Rainfall patterns

Step, impulse and ramp-type rainfall patterns are valuable for investigating the time varying characteristics of infiltration. On the other hand, the simulator can supply step type rainfall. Therefore, step type rainfall was mainly used. **Table 4** shows the rainfall patterns which were used in the experiments.

Table 2
Experimental Soils.

	Symbol	Name	Producing Field	Compaction	Comments
Sandy soils	S1	Coarse Sand (0.5-2.0mm)	Kashima*	No	Different Particle size
	S2	Fine Sand (-0.5mm)	Kashima*	No	
	L	Kanto Loam	Sakuramura*	Vibrator every 20cm	Contrast with sands
	K	Kanuma Pumice	Kanuma**	No	Skeleton of particle
Loamy soils	L1	Humic Loam	Sakuramura*	Foot every 20cm	Skeleton of particle
	L2	Compacted Loam	Sakuramura*	Vibrator every 20cm	Different compaction
	L3	Uncompacted Loam	Sakuramura*	Foot every 20cm	
	L4	Stratified Loam	Sakuramura* Kashima*	Foot every 20cm	Two layers

*Ibaraki Prefecture
**Tochigi Prefecture

Table 3
Particle Size Distribution of Soils.

Soils \ Particle size	mm -0.074	mm 0.074-0.42	mm 0.42-2.0	mm 2.0-
S1	1.0%	6.8%	92.2%	0.0%
S2	2.0	82.0	15.8	0.2
L	31.9	37.9	30.2	0.0
K	1.1	3.3	25.9	69.7
L1	34.8	28.8	26.4	10.0
L2	37.6	18.5	28.4	15.5
L3	31.9	16.3	32.4	19.4
L4*	31.2	17.3	29.3	22.2

S1, S2, L, K are measured in 1977,9.
L1, L2, L3, L4 are measured in 1979,1.
*Upper layer

Table 4
Rainfall Inputs Used in the Experiments.

Type	Intensity *Duration	Pattern	1977 June	1977 Nov.	1978 Apr. May	1978 Aug. Sept.
Step	15mm/h* 6h				o	o
	30mm/h* 2h		o	o		
	30mm/h* 4h			o		
	30mm/h* 6h				o	o
	50mm/h* 1h					o
	50mm/h* 2h		o	o		
	50mm/h* 6h				o	o
	70mm/h* 2h		o			
	100mm/h* 2h		o			
Impulse	100mm/h*.5h				o	o
Staircase	30mm/h* 1h +70mm/h* 1h				o	o
Alternating rectangular	50mm/h*.5h for 3 times				o	o

(4) **Measurements.**

In order to trace infiltrating water from the surface to the ground water level, three kinds of water content measurements in the vertical soil sections and measurement of the ground water discharge were performed.

Water content

a. Specific resistance

Specific resistance is inversely proportional to the water content of soil, i. e. when the water content increases the specific resistance decreases.

b. Neutron scattering

A neutron scattering meter, based on the principle that attenuation of fast neutrons in soil is proportional to the hydrogen content of the soil, was used for measurement of the soil water content.

c. Soil moisture potential

A tensiometer was used to measure the matric suction of soil-water which is the pressure head for water movement.

Ground water flow

d. Amount of ground water discharge

Using a tipping bucket-type flow meter, the flow of ground water through the models was measured.

e. Ground water level

In the experiments, the level of the ground water was fixed in the soils (see **Fig. 2**), so there were no inflow of air from the bottom of soils.

The location of sensors is shown in **Fig. 2**.

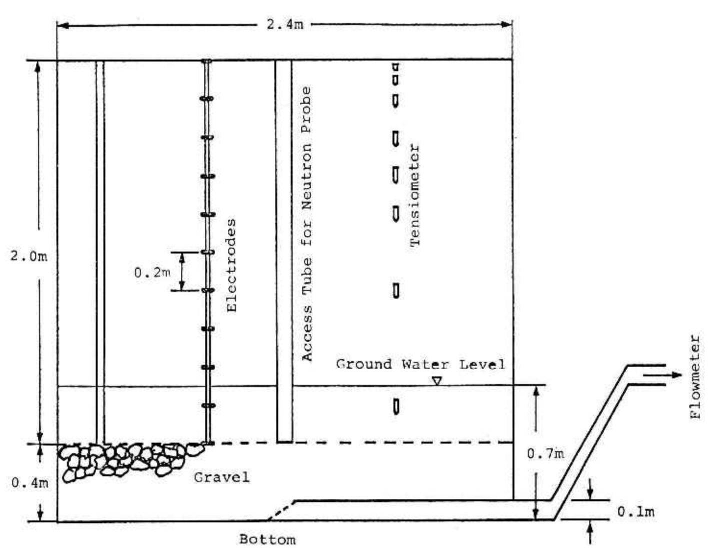

Fig. 2 Location of Sensing Elements.

(5) Interval of measurements

From data of the Kumamoto area, in Kyushu Island, Southern Japan, the peak of rainfall precipitation is observed in June, and the peak of the ground water level occurs in September at about 80m depth from the surface of the ground. Although increase of the ground water level is not always affected by precipitation, the apparent velocity of downward infiltration is about 0.9m/day. So, periods of 5 minutes to 1 hour were chosen for the measurements of the specific resistance and the soil moisture potential, and those of 30 minutes to several hours were chosen for the measurement of neutron scattering.

4. Specific resistance and rapid changes of soil-water content

In this chapter, the measurement of specific resistance to indicate the water content is considered. When the soil-water content is high, the specific resistance is low. Above phenomenon is utilized in measurement. The theory of specificr esistance is simple, and this method does have some merits for hardware and software in application.

(1) Theory of specific resistance

Measurement of specific resistance has been widely used to survey structures of strata. For practical measurement, electrodes are set in line on the surface of the ground. Electric fields can be induced widely in the ground, so specific resistance of large objects, such as the ground, may be easily measured. There are no restrictions on the size of the object in terms of the theory, so measurement of the specific resistance of the semiconductors has been reported (Mac Donald, 1953). As for resistance of the ground, Rhoades (1976) designed probes and measured the salinity of the ground. In his experiment, probes were located in a vertical line, and four neighbouring electrodes were used to measure the specific resistance of the ground.

The relation of specific resistance and water content in soil has been discussed by Katsurayama (1957) in measurements concerned with the water content of soil in fields, and by Yamashita (1971) to evaluate the formation resistivity factor of sedimentary rock. They both analyzed specific resistance in rectangular portions of soil. Katsurayama applied his results directly to measure the soil-water content using porous blocks. He measured resistance (Ω) and not specific resistance (Ωm), however. The results for the measured resistance are affected by the location and the size of the electrodes of the sensing blocks, so merits of specific resistance measurement were not realized in this application. The author has developed a theory (1980) for measuring the specific resistance for the water content of any soil type and soils of any size whereby a general soil structure postulated. The theory is summarized below.

On any closed surface in the soil, which is composed of soil particles, air and water, the ratio of the area occupied by each of materials to the total area is uniform for each material. Thus the apparent specific resistance of the soil is,

$$\frac{1}{\rho}=\frac{N_s}{\rho_s}+\frac{N_a}{\rho_a}+\frac{N_w}{\rho_w} \qquad (1)$$

$$\text{and} \quad N_s + N_a + N_w = 1$$

where ρ is the apparent specific resistance, ρ_s, ρ_a, ρ_w are the specific resistances of the soil particles, air and water, and N_s, N_a, N_w are the ratios of area occupied by the soil particles, air and water to the total area of the closed surface. The above relation can be reduced to the following simple equation, when the specific resistance of soil particles and air are larger than that of water,

$$\frac{1}{\rho} = \frac{N_w}{\rho_w} \tag{2}$$

Moreover, N_w can be shown to be the ratio of the volume of water to the total volume of the closed surface.

In application of this theory, there is no need to use porous blocks. The four electrodes method can be used to measure the specific resistance of the soil directly. The effect of time lag which cannot be neglected when using porous blocks is eliminated.

(2) Characteristics of specific resistance for measuring soil-water content

There are two kinds of methods to measure the water content of soil. One is a direct method in which the weight loss of the soil after drying indicates the water content of the soil. The other is the indirect method in which variables, affected by the water content of soil, are measured and the water content of the soil is acquired by calibration. In the direct method, it is necessary to remove the soil sample for measuιement, and the state of the ground is inevitably disturbed. Moreover techniques for removing soil samples may affect wateι content, and error in the measured value cannot be ignored. Therefore, indirect methods are widely adopted in fieled use, when it is not permissible to disturb the ground conditions or continuous measurement is needed.

Here, the characteristics of the specific resistance method are discussed.

a. As sensing elements, electrodes are used. Electrodes are generally made of metal, so they are easy to use and lay in the ground in comparison with the ceramic cup of the tensiometer. After laying in the ground additional maintenance is usually not required except for cables.

b. There are generally no restrictions in selecting materials and shapes of electrodes, and many sensing elements could be used in the present expeιiments.

c. Specific resistance is affected by some parameters, especially by the ionic content of water. Water is electrolytic, and may by polarized when an electric field is induced. The apparent specific resistance is rather high when the electric field is induced than the one when the field is not induced. This may restrict **a.** and **b.** mentioned above.

d. With suitable instrumentation, such as the rotary switch, specific resistance of many points can be measured in a short period of time. In the present experiments, it required 3 minutes for 32 measuring points. This is equal to about 6 seconds per measurement. Therefore, the time-varying changes of the soil-water content can be measured. Generally speaking, it takes a certain time for most methods to attain equilibrium conditions, for example, the ceramic porous cup requires about 10–30 minutes. As for the present experiments, the soil-water content is affected by the time-varying rainfall intensity, and the ground water discharge depends on the content, too. This means that the condition of water distribution in the ground at every depth must be measured in minutes. The requirement for fast measurement, as mentioned above, may restrict some methods.

e. Methods for measurement of electrical variables are well-established, so optimal and automatic measurement systems can be devised. In the present experiments, only one person was required for measurement of the specific resistance. It seems that one person at least is required to observe the state of measuring system, if trouble develops.

f. When the four electrodes method is used to measure specific resistance, the measured value represents the specific resistance of a certain spatial volume of soil, and is affected by the spatial distribution of specific resistance surrounding the electrodes. This method is fundamentally different from the method which measure electrical resistance (Ω) at one point in the ground using porous blocks. The size of area which affects the measurement is dependent on the separation distance between the electrodes. The area becomes small when the separation distance is small. The ground in which infiltrating water must be measured is usually so large that measurement at a point such as the pore pressure measurement, by means of porous cups, does not give a representative value for the ground. Therefore the four electrodes method mentioned above is favourable when the object for measurement is large.

(3) Method of measurement

Fig. 3 shows the location of electrodes for measurement of specific resistance in detail. Electrodes, which were made of brass and 3 mm in diameter, were fixed at intervals of 20 cm on vinyl chloride pipe, which was 18mm in diameter. The upper first electrode was located at the surface of the ground models. The neighbouring four electrodes were used for one measurement. Using a rotary switch, current electrodes and potential electrodes for every depth of the ground can be chosen in succession. The current output of the ground specific resistance meter (YEW, 3244) supplied an electrical motive force for inducing electric field in the ground, The output is an alternating square wave generated by the transistor inverter circuit. The input voltage to the inverter circuit is usually 12V DC. In this type of circuit, the output frequency decreases when the input voltage to the inverter becomes low. So the input voltage was fixed at 12V DC using a regulated power supply (CEC, 505A), and the frequency was maintained at 34Hz for the experiments.

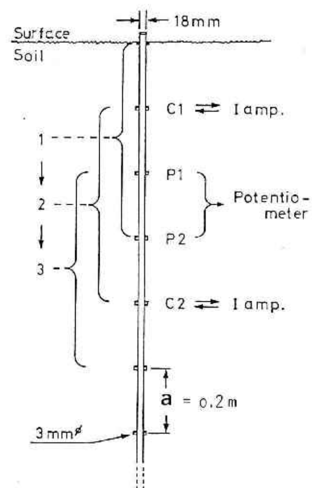

Fig. 3 Location of Electrodes for Measurement of Specific Resistance.

Specific resistance was calculated by computer (HP, 9825A), using the values of alternating veltage between the potential electrodes and that of current supplied by the current electrodes as measured by a digital voltmeter (HP, 3455A). The alternating signals were measured by the digital voltmeter which measures the 'true-RMS value' of the signal. The alternating current was transformed into voltage by a resistance about 1 ohm. The value of the resistance was measured at any time in the experiments. **Photo 2** and **Fig. 4** show equipment and schematic for the measurement of specific resistance.

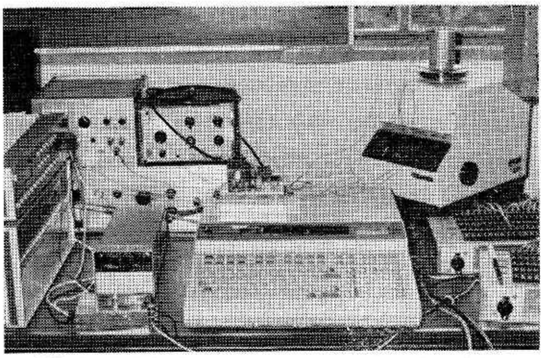

Photo 2 Equipment for Measuring Specific Resistance.

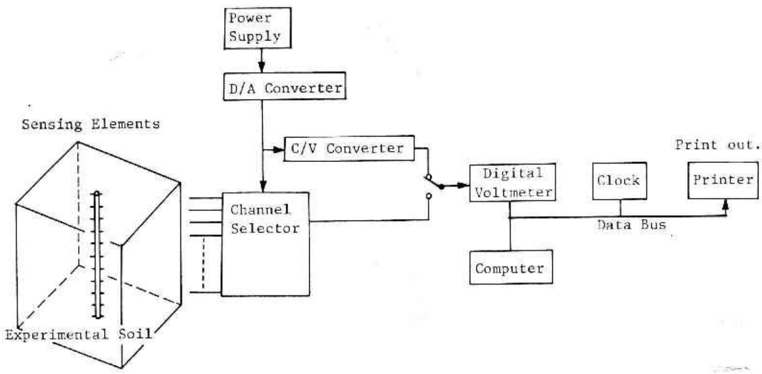

Fig. 4 Schematic of Measurement of Specific Resistance.

In **Fig. 3**, C1 and C2 are the current electrodes from which $+I$ and $-I$ ampere of current flow alternately at a frequency of 34 Hz. P1 and P2 are the potential electrodes. The electrodes stretch out from both side of the pipe, so that the electric field is induced spherically with the current electrodes as the centers. When the specific resistance of the ground is uniform, it is expressed as,

a. when Cl is located at the surface of the ground,

$$\rho=\frac{8\pi a}{3}\times\frac{V}{I} \tag{3}$$

b. when Cl is located under the surface,

$$\rho=4\pi a\times\frac{V}{I} \tag{4}$$

where, $\rho(\Omega \mathrm{m})$ is the apparent specific resistance, $V(\mathrm{V})$ is the voltage between P1 and P2, $I(\mathrm{A})$ is the induced current and $a(\mathrm{m})$ is the separation distance of the electrodes. In the present paper, specific resistance was calculated by use of the above equations. Specific resistance is affected by the spatial distribution of the soil-water content around the electrodes. Therefore, it is difficult to say that the measured value represents a value for a specific point in the ground. In the present paper, the value was treated as the one at the center point of the electrodes P1 and P2. The value nearest to the surface was treated in the same way as the one 30cm below the surface. Therefore, it seems that the specific resistance became low immediately after rain is supplied to the surface. According to the method of data processing mentioned above, change of the specific resistance is shown as that of the point, 30cm under the surface.

(4) Theory of data processing

It is difficult to decide whether the sensing elements are well located in the soil to detect changes of water content. For example, porous blocks are frequently used to make infiltrating water move in the blocks at the same speed as in the soil surrounding the blocks. The state of contact between the sensing elements and the soil affects the measured values of specific resistance. In the present experiments, the electrodes were laid in soil at the same time as the experimental soil was filled. The electrodes were wetted with water so as to attain better contact conditions. Although these procedures were taken, it is difficult to determine whether the conditions adopted were optimum, i. e. whether the current flow from the electrodes is spherical or not. Therefore, in the present paper, the following procedure was adopted to investigate the movement of water flow.

If the condition of compaction of soil around the electrodes is not uniform, the current density does not have the same value at all points on the spherical surface whose center is represented by the current electrode. Even for this condition, the shape of the current distribution does not change, unless the relative location between the electrodes and the soil changes. And the current density induced in the soil is proportional to the total current which flows from the current electrodes.

Therefore, the current density $\boldsymbol{J}(\boldsymbol{r})$ $(\mathrm{A/m^2})$ at any point $\boldsymbol{r}$ in soil may be expressed as,

$$\boldsymbol{J}(\boldsymbol{r}) = I\,\boldsymbol{C}(\boldsymbol{r}) \tag{5}$$

where I (A) is the total current and $\boldsymbol{C}(\boldsymbol{r})$ $(\mathrm{m^{-2}})$ is the shape of the current distribution.

$\boldsymbol{C}(\boldsymbol{r})$ is a function of $\boldsymbol{r}$, and is not affected by the total current. The potential difference V (V) between any two points $\boldsymbol{r}_1$, $\boldsymbol{r}_2$ is expressed as,

$$V = \rho\int_{r_1}^{r_2} \boldsymbol{J}(\boldsymbol{r})\cdot \mathrm{d}\boldsymbol{r} = \rho I\int_{r_1}^{r_2} \boldsymbol{C}(\boldsymbol{r})\cdot \mathrm{d}\boldsymbol{r} \tag{6}$$

If the specific resistance at a time t_0 is expressed as ρ_0 and at the time t_1 as ρ_1, the ratio of ρ_1 to ρ_0 becomes,

$$\frac{\rho_1}{\rho_0} = \frac{\left(\frac{V}{I}\right)_{t_1} \Big/ \int_{r_1}^{r_2} \boldsymbol{C}(\boldsymbol{r})\cdot \mathrm{d}\boldsymbol{r}}{\left(\frac{V}{I}\right)_{t_0} \Big/ \int_{r_1}^{r_2} \boldsymbol{C}(\boldsymbol{r})\cdot \mathrm{d}\boldsymbol{r}} = \frac{\left(\frac{V}{I}\right)_{t_1}}{\left(\frac{V}{I}\right)_{t_0}} \tag{7}$$

The above relation means that the ratio of the measured specific resistance at any time to the one at some time is independent of the shape of the current distribution.

On the other hand, from the **Eq. 2** and **Eq. 7** the following relation is obtained.

$$\frac{\rho_1}{\rho_0}=\left(\frac{N_w}{\rho_w}\right)_{t_0}\left(\frac{\rho_w}{N_w}\right)_{t_1}$$

If the specific resistances of watei at t_0 and t_1 have the same value, the above relation becomes,

$$\frac{\rho_1}{\rho_0}=\frac{(N_w)_{t_0}}{(N_w)_{t_1}} \tag{8}$$

This means the ıatio of specific resistance equals the inverse ratio of the water content of soil.

Eq. 7 and **Eq. 8** mean that even if the current distribution around the electrodes is not uniform, the ratio of specific resistance which is derived fıom **Eq. 3** and **Eq. 4** equals the inverse ratio of water content of soil.

As the value of ρ_0, the specific resistance of before experiment is chosen, the following criteıia are adopted:

a. If the specific resistance at any point in the soil begins to decrease, the wetting front has reached the particular point.

b. If the vertical distıibution of specific resistance has reached equilibrium, i. e. where individual values for specific resistance do not change, the distribution of water content is also in equilibrium, too.

According to the above criteria, a graph of specific resistance (denoted by ⓑ) and a contour map (denoted by ⓐ) of the normalized specific resistance divided by the value for the before experimental measurement are made. From these graphs and ground water flow (denoted by ⓒ), the time-varying response of specific resistance to precipitation of rainfall, which includes movement of wetting front, attainment of equilibrium, growing of capillary fringe, ground water discharge and drying condition of soil after precipitation has ended, can be traced for all experimental soils.

5. Results of experiments and discussion

All of the experiments are shown in **Table 1** In this section, some characteristic results of the experiments are discussed. First, the results for the experiments of sandy soils through which water readily infiltrates are discussed. Secondly, the results for the experiments of loamy soils in which it is not easy for water to infiltrate are discussed. Each discussion is treated according to the patterns of rainfall input, step-type rainfall and alternating rectangular-type rainfall. The step-type of rainfall seldom occurs in the natural world, but the response makes it easy to investigate transient and stationary states of infiltration. The rectangular-type of rainfall is a model for natural rainfall. In the following sections, the results are described and discussed, mainly using data of specific resistance. Technical terms used in these sections are defined as follows: In **Fig. 5**, the wetting zone, existing above the wetting front, is the zone where the capillary force is acting. The volume of water decreases with depth in the wetting zone. The transmission zone is where the volume of water is nearly uniform when

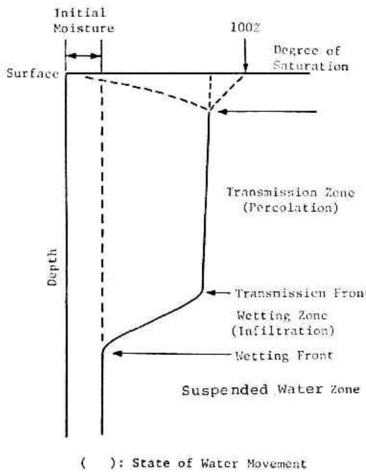

Fig. 5 Terms of Infiltrating Water.

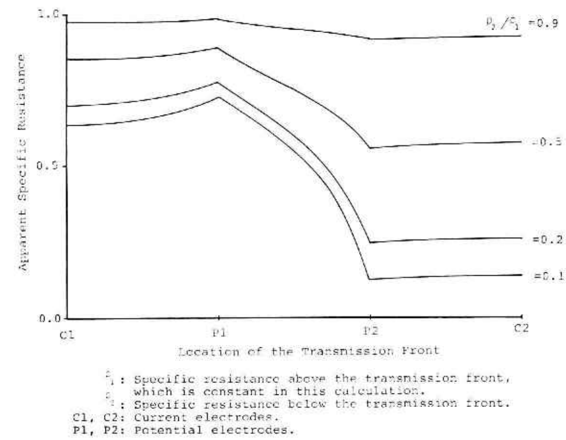

Fig. 6 Changes of the Apparent Specific Resistance.

rain is supplied constantly on the ground surface. The transmission front is the boundary between the transmission zone and the wetting zone. In other words, infiltrating water and air change their locations among the soil particles below the transmission front. Above the transmission front, this kind of change may not occur.

If the thickness of the wetting zone is so thin that the transmission zone and the suspended water zone are separated sharply by the wetting front, as observed in sand, then the potential difference between P1 and P2, in **Fig. 3**, is expressed as,

a. when the wetting front is located between Cl and P1,

$$V=\frac{\rho_1 I}{4\pi a}\left[\frac{\rho_2}{\rho_1+\rho_2}+\frac{1}{2}+\frac{\rho_1-\rho_2}{\rho_1+\rho_2}\frac{1}{(5-2\varepsilon)(4-2\varepsilon)}\right] \tag{9}$$

b. when the wetting front is located between P1 and P2,

$$V=\frac{I}{4\pi a}\left[\frac{\rho_1{}^2+\rho_2{}^2}{\rho_1+\rho_2}-\frac{\rho_1-\rho_2}{\rho_1+\rho_2}\left(\frac{\rho_1}{3-2\varepsilon}-\frac{\rho_2}{1+2\varepsilon}\right)\right] \tag{10}$$

c. when the wetting front is located between P2 and C2,

$$V=\frac{\rho_2 I}{4\pi a}\left[\frac{\rho_1}{\rho_1+\rho_2}+\frac{1}{2}-\frac{\rho_1-\rho_2}{\rho_1+\rho_2}\frac{1}{(3+2\varepsilon)(2+2\varepsilon)}\right] \tag{11}$$

where ρ_1 is the specific resistance of soil under the wetting front, ρ_2 is that above the wetting front, a is the separation distance between the electrodes, εa is the distance between the wetting front and the nearest electrode above the wetting front.

The change of the apparent specific resistance, when the wetting front goes down, is shown in **Fig. 6**. The boundary can be detected easily from data of specific resistance, so movement of the boundary, i. e. the transmission front, is used to evaluate the velocity of the wetting front in the following sections.

(1) Results for sandy soils (S1,S2,K)

A. Step-type rainfall.

Fig. 7, 8, 9 and **Fig. 10, 11, 12** give the results for **S2** (fine sand) and **K** (Kanuma pumice) respectively.

Result 1.

The velocity of the transmission front (see **Fig. 5**) increased when rainfall became intense. In each figure, ⓐ represents the contour map of normalized specific resistance. The contour lines drawn from the surface of the ground to the inner part with lapse of time show that the specific resistance at each depth decreased with the increase of infiltrating water from rainfall. In other words, the transmission front, to say nothing of the wetting front, had reached the particular point of the ground. The inclinations of the contour lines of **Fig. 7, 8, 9** show that the velocity of infiltration increased when rainfall became intense for **S2** (fine sand). As in the case of **S2**, **Fig. 10, 11, 12** show the same phenomenon for **K** (Kanuma pumice).

Discussion.

Table 5 shows several characteristics of the downward movement of the transmission front: the velocity of the transmission front (**V**), the time lag from the beginning of rainfall till the time when the transmission front reached −20cm from the surface of the ground (**T**), the accumulation of rainfall for the duration mentioned above (**R**) and the value of intensity of rainfall divided by the velocity of the transmission front (**A**), in each section.

S1 (coarse sand) and **K** (Kanuma pumice) showed similar velocities of infiltration.

Table 5 Movement of Transmission Front.

Soils / Intensity	Sandy soils S1	S2	L3	K	Loamy soils L1	L2	L3	L4	
15mm/h*6h	V= 0.44	0.36	0.50	0.36	0.36	0.42	0.48	0.39	
Sand 20mm/h*	T=80	161	72	112	70	71	42	82	
Loam 15mm/h*	R=26.7	53.7	24.0	37.3	17.5	17.8	10.5	20.5	
	A= 7.6	9.3	6.7	9.3	6.9	6.0	5.2	6.4	
30mm/h*6h	V= 1.00	0.52	1.20	0.88	0.35	0.83	0.52	1.00***	(1.23)
Sand 33mm/h*	T=31	75	33	43	40	51	22	30	
Loam 41mm/h*	R=17.1	41.3	18.2	23.7	27.3	34.9	15.0	20.5	
	A= 5.5	10.4	4.6	6.3	19.5	8.2	13.1	6.8	(5.6)
50mm/h*6h	V= 1.32	0.92	0.88***	1.33	0.25***	1.00***	0.86***	0.78***	(1.67)
Sand 58mm/h*	T=25	41	42	28	70	51**	32	22	
Loam 63mm/h*	R=24.2	39.7	40.7	27.1	73.0	53.2	33.4	23.0	
	A= 7.3	10.5	12.1	7.3	42	10.5	12.2	13.5	(6.3)

V(cm/min): Velocity of the transmission front.
T(min) : Time lag from beginning of rainfall until the transmission front reached -20cm from the surface of the ground.
R(mm) : Accumulation of rainfall in the period of T.
A(%) : Rainfall intensity divided by V.
* : Actual intansity.
** : Time lag until the transmission front reached -40cm.
*** : Values around the surface area.
( ) : Values in the lower layer.

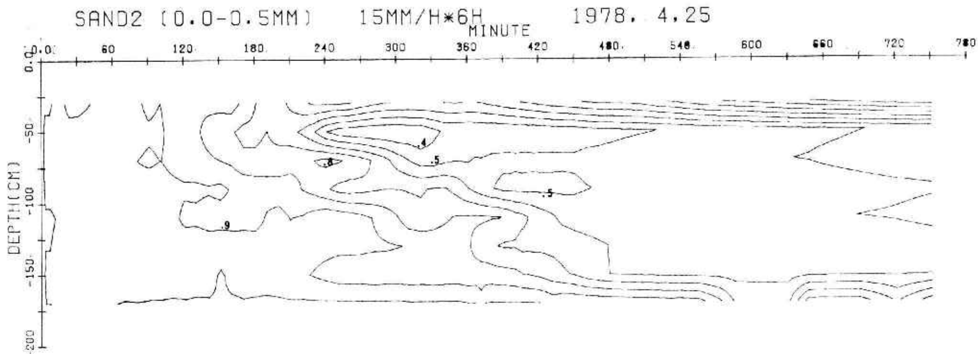

ⓐ Contour Map of Normalized Specific Resistance (see section 4-(4)).

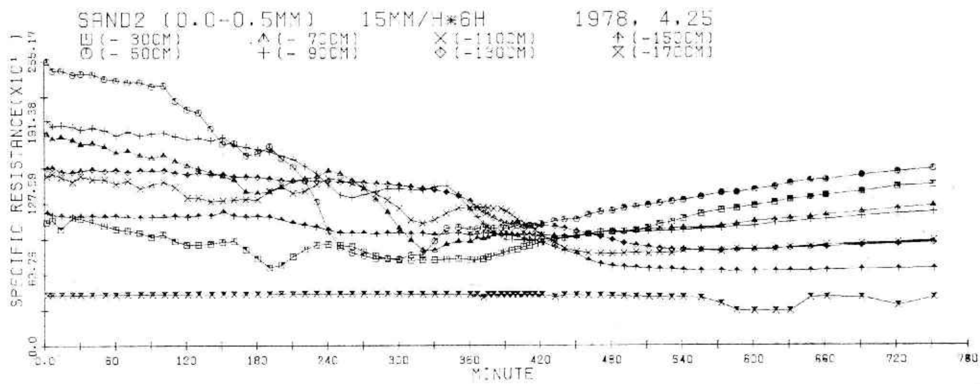

ⓑ Specific resistance curves showing time-varying vertical distribution of water content.

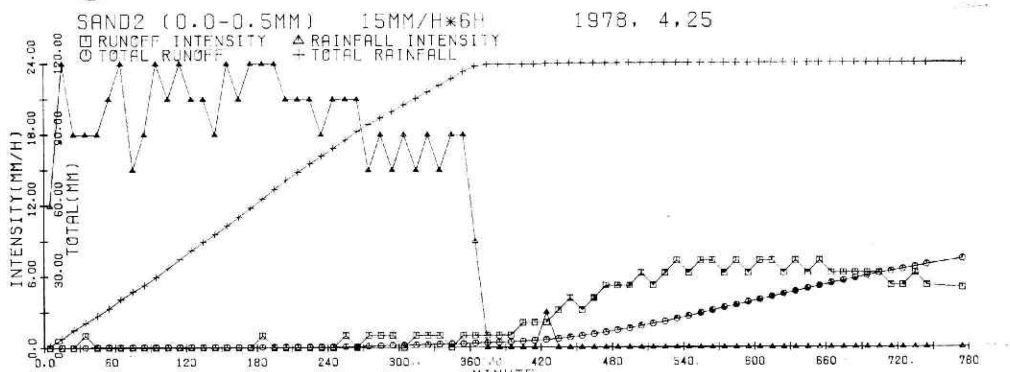

ⓒ Intensity of Rainfall and Discharge of Ground Water.

Fig. 7 Fine Sand (S2), 15mm/h for 6 hours.

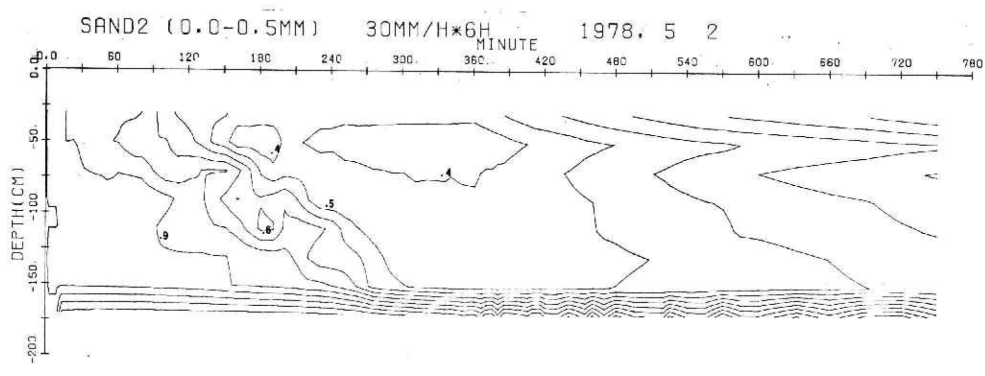

ⓐ Contour Map of Normalized Specific Resistance (see section 4-(4)).

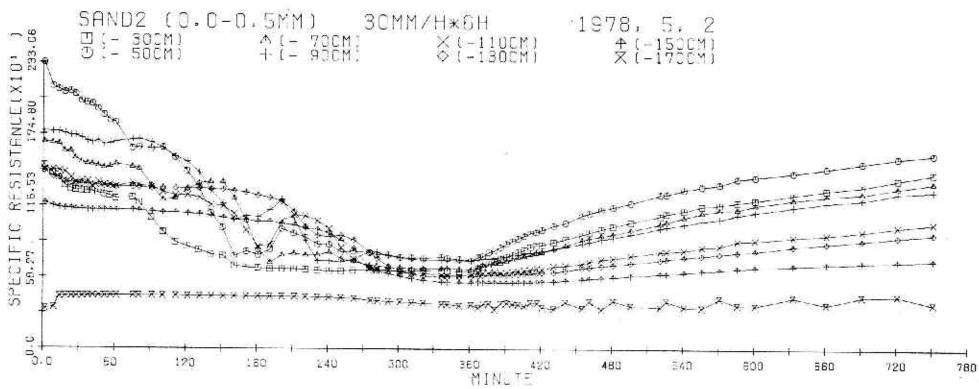

ⓑ Specific resistance curves showing time-varying vertical distribution of water content.

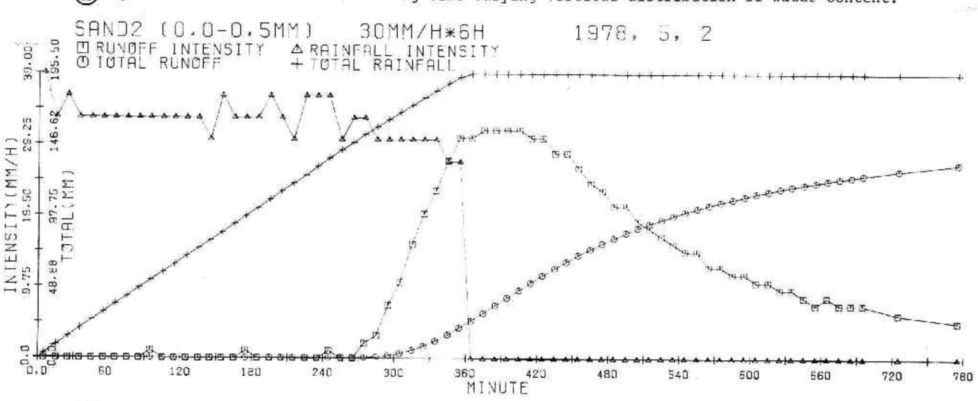

ⓒ Intensity of Rainfall and Discharge of Ground Water.

Fig. 8 Fine Sand (S2), 30mm/h for 6 hours.

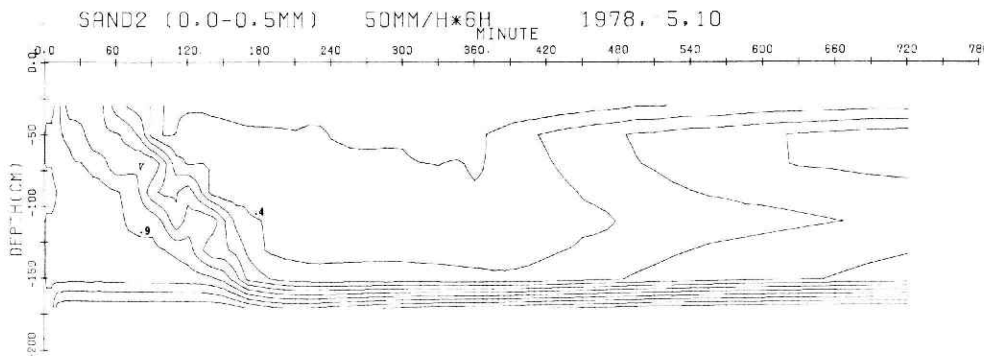

ⓐ Contour Map of Normalized Specific Resistance (see section 4-(4)).

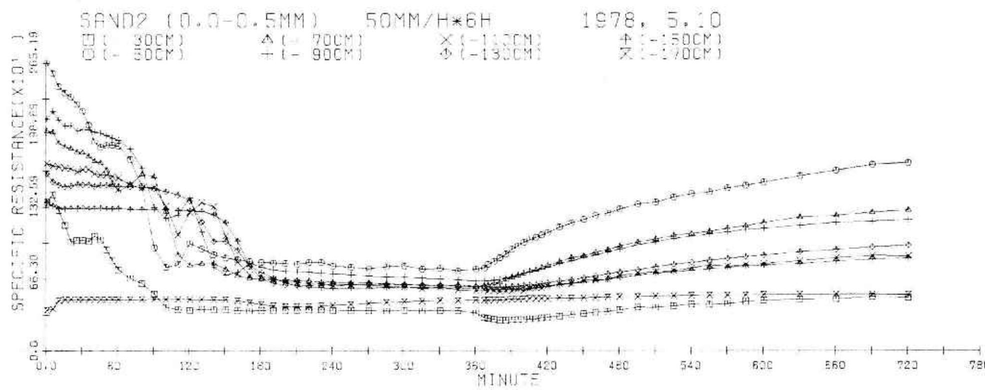

ⓑ Specific resistance curves showing time-varying vertical distribution of water content.

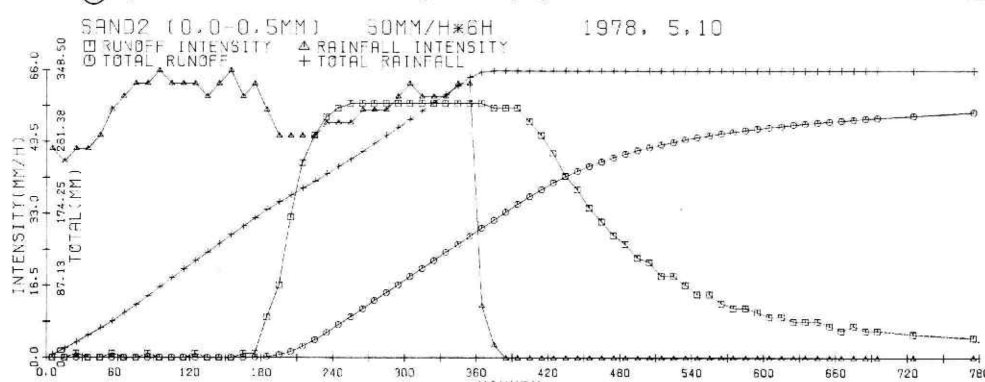

ⓒ Intensity of Rainfall and Discharge of Ground Water.

Fig. 9 Fine Sand (S2), 50mm/h for 6 hours.

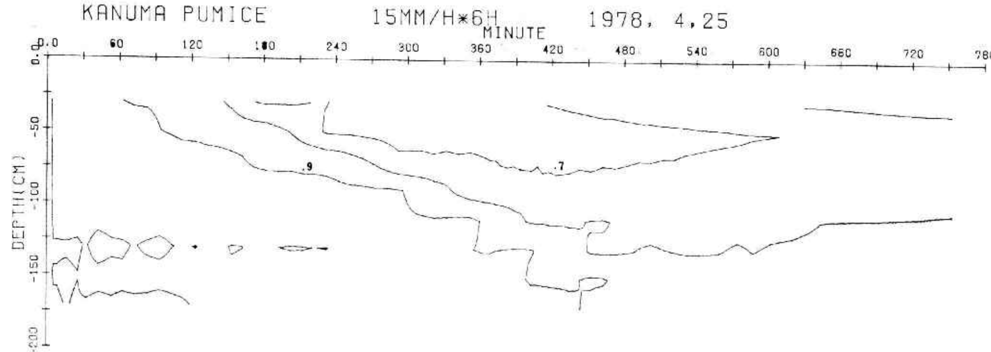

ⓐ Contour Map of Normalized Specific Resistance (see section 4-(4)).

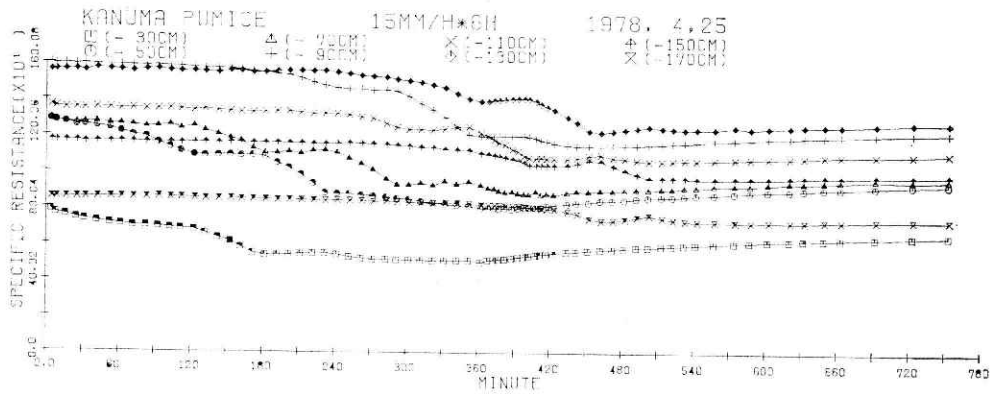

ⓑ Specific resistance curves showing time-varying vertical distribution of water content.

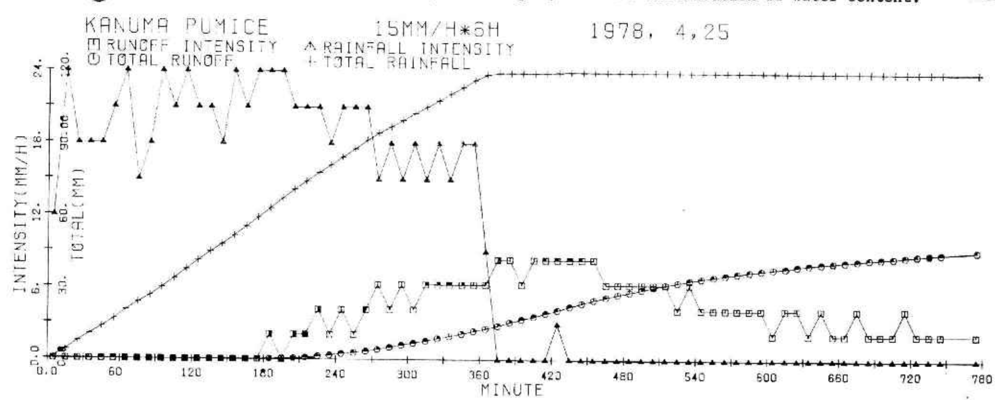

ⓒ Intensity of Rainfall and Discharge of Ground Water.

Fig. 10 Kanuma Pumice (K), 15mm/hor 6 hours.

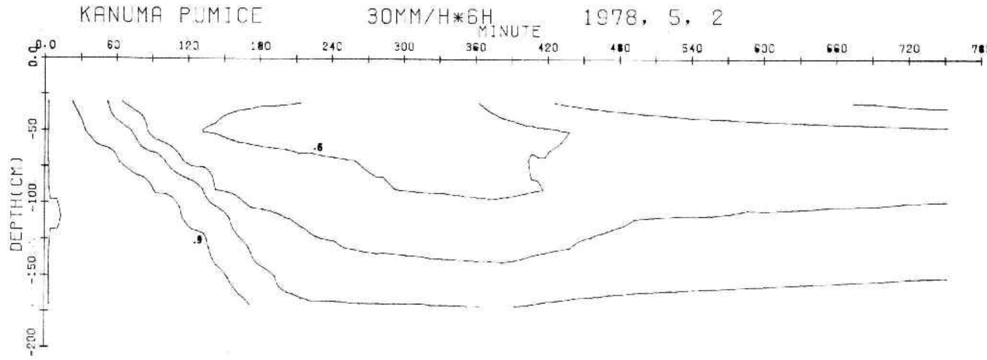

ⓐ Contour Map of Normalized Specific Resistance (see section 4-(4)).

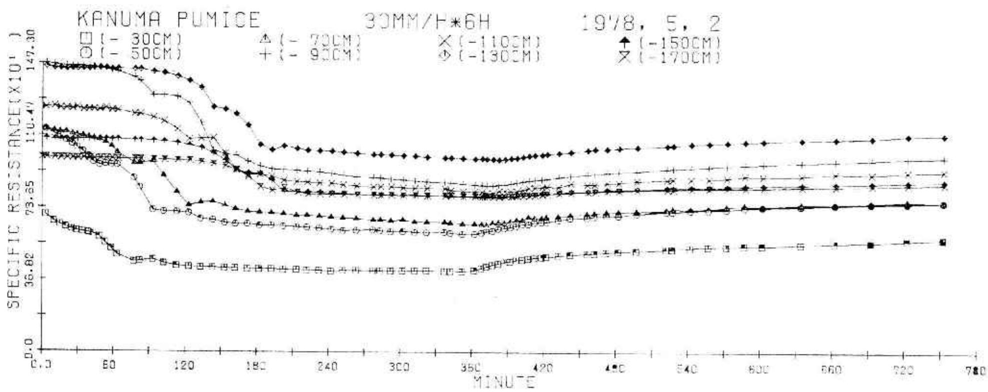

ⓑ Specific resistance curves showing time-varying vertical distribution of water content.

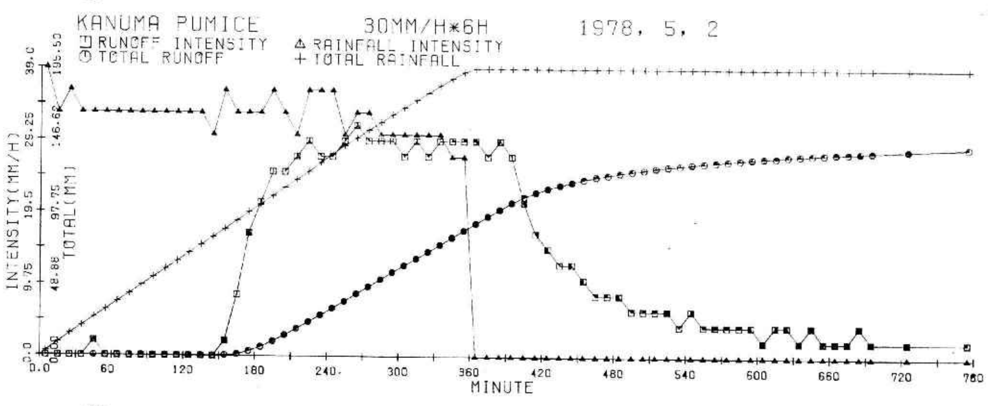

ⓒ Intensity of Rainfall and Discharge of Ground Water.

Fig. 11 Kanuma Pumice (K), 30mm/h for 6 hours.

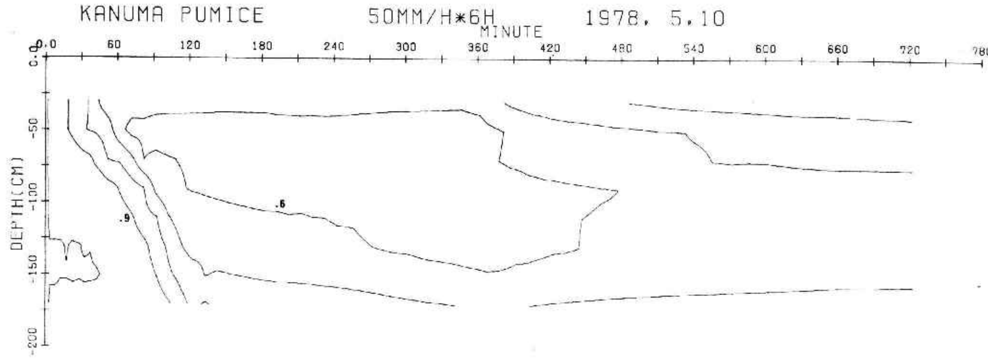

ⓐ Contour Map of Normalized Specific Resistance (see section 4-(4)).

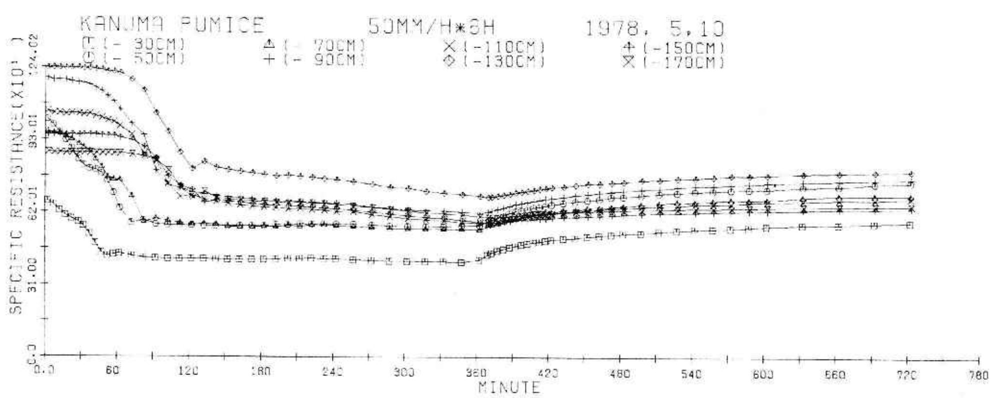

ⓑ Specific resistance curves showing time-varying vertical distribution of water content.

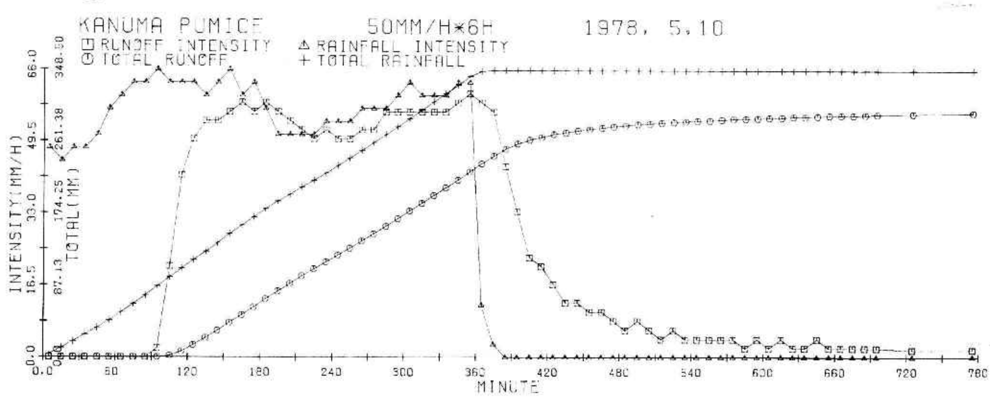

ⓒ Intensity of Rainfall and Discharge of Ground Water.

Fig. 12 Kanuma Pumice (K), 50mm/h for 6 hours.

Velocities for **S2** (fine sand) were rather slow. Each velocity increased when rainfall became intense.

Near the surface of the ground, the following phenomena were observed,

a. **T** for **S1** (coarse sand) was smaller than that for **K** (Kanuma pumice), and the difference of these values decreased when rainfall became intense.

b. **R** for **S1** (coarse sand) varied whithin 17–27mm, that for **S2** (fine sand) 40–53mm and that for **K** (Kanuma pumice) 24–37mm. These values were similar for the particular soils for the different intensity of rainfall.

c. The soil-water had been redistributed giving an equilibrium condition until the beginning of the following experiment. That is to say, drainage of the soil-water under gravity had finished.

From these observations, the water from rainfall at the beginning of the experiment is supposed to fill voids near the surface of the ground, where soil-water has evaporated and the area shows a smaller water content than that of the inner part of the ground. According to the result **a** and **b**, some quantity of water must be stored in voids around the surface before the transmission front passes the -20cm point under any intensity of rainfall. The depth of -20cm is an arbitrary value. In the experiments, the electrodes were set at this point, so -20cm is chosen as the observing point of infiltration.

After completion of storage at the surface, the transmission front begins to move downward. **A** in **Table 5** is the value of rainfall intensity divided by the velocity of the transmission front. These values are almost equal for each soil under any intensity of rainfall. Considering result **b**, mentioned above, it is supposed that water infiltrates in a downward direction adding some amount of water to the previously existing water in the soil. From another point of view, a uniform amount of water depending on the types of soil is added to the existing water in the soil, when the transmission front moves dewnward. Therefore the velocity of movement of the transmission front increases with increase of intensity of rainfall.

(see Result 4 for the permeability of infiltration.)

Result 2.

The infiltration at each depth reached equilibrium with transit of the transmission front under constant and continuous rainfall. The specific resistance did not change at each depth after the transmission front reached the level of the ground water, in **Fig. 8**ⓑ, **9**ⓑ and **11**ⓑ, **12**ⓑ. This means that the soil-water content was time-invariable for each depth, and that the amount of water supplied from the upper part and discharge to the lower part were equal. This equilibrium condition occurred at every part of the soil.

Discussion.

Fig. 8ⓒ, **9**ⓒ and **Fig. 11**ⓒ, **12**ⓒ show the intensity and the accumulation of discharge in addition to the rainfall intensity and the accumulation of rainfall. The period when the intensity of the discharge is in equilibrium, is in accordance with the equilibrium of the specific resistance mentioned above. On close inspection of the results of the specific resistance around the time when infiltration reached equilibrium in ⓑ of each figures, low uniform values were successively obtained from the uppur to the lower parts, and finally infiltration reached equilibrium in every part of the ground. In the equilibrium condition, infiltration turns into percolation, as shown in **Fig. 5**. It is considered that the equilibrium condition appears after transit of the transmission front. Therefore, the earlier thefront appears at the point −20cm and the faster the velocity of infiltration becomes below the point −20cm, the earlier the state of infiltration reaches equilibrium.

Result 3.

Discharge of the ground water began before the transmission front reached the level of the ground water. Contour maps of **Fig. 7**ⓐ, **8**ⓐ, **9**ⓐ and **Fig. 10**ⓐ, **11**ⓐ, **12**ⓐ and the intensity of the discharge shown in ⓒ of each figure, show the discharge began before the transmission front reached the ground water level.

Discussion.

The time at which the discharge began (**U**) and the position of the transmission front at this time (**H**) are shown in **Table 6**. The time at which the discharge of the ground water began became early with increase of rainfall intensity, and the location of the transmission front at that time were almost equal in the experiments for each soil type (**S1**, **S2**, **K**). Concerning the reason why the discharge began before the arrival of the transmission front to the ground water level, it is considered that the wetting front reached upper bound of the capillary fringe. This means that pressure propagates through the capillary water to the ground water level, and the ground water flows out. Therefore, the transmission front is considered as locating at the upper part

Table 6 Beginning of Ground Water Discharge.

Soils / Intensity	Sandy soils S1	S2	L3	K	Loamy soils L1	L2	L3	L4
	**	**		**		**	**	**
15mm/h*6h	U=165	255	285	185	275	155	215	165
Sand 20mm/h*	265	345		205		185	235	205
Loam 15mm/h*	H=112	116	44	124	76	115	67	117
	68	84		117		102	57	102
30mm/h*6h	U=145	275	105	155	125	135	105	105
Sand 33mm/h*								
Loam 41mm/h*	H= 36	43	64	52	120	80	107	69
50mm/h*6h	U=115	165	75	95	105	85	75	35
Sand 58mm/h*								
Loam 63mm/h*	H= 32	36	124	61	141	96	113	140

U(min): Commencing time of the ground water discharge.
H(cm) : Height of the transmission front above the ground water level.
* : Actual intansity.
** : (upper) Commencing time, (lower) Intensity of discharge began to increase.

of capillary fringe at the beginning of the ground water discharge (see Appendix). The location of the transmission front **H** at the beginning of the ground water discharge **U** was different for each soil. The location **H** in **S1** (coarse sand) was lowest, that in **S2** (fine sand) medium, and the one in **K** (Kanuma pumice) highest. The capillary rise reached a high level for loamy soils, but not sandy soils as the experiments went on. This was caused by the difference of the water retaining characteristics of each seil. The distribution of the soil-water content before each experiment was that there existed only suspended water which did not move under gravity. Therefore, the capillary water reached particular height for each soil in this condition, and it was equal for each experiment.

The schematic of the time-varying water potential and the beginning of the discharge are shown in Appendix.

Result 4.

The permeability of percolation at the equilibrium condition was similar to the one of saturated infiltration, where the percolation is defined in **Fig. 5**. It is difficult to propose a physical model of unsaturated infiltration for rainfall, In the present section, permeability of percolation is derived by postulating that the percolation was performed by the type of 'Open system-Unsaturated-Capillary-Percolation' which was studied by Nakamura (1969).

Discussion.

The 'Open system-Unsaturated-Capillary-Percolation' means that water percolates through the capillary, and the capillary water is surrounded by air which is open to outside air through the surface of the ground. For convenience of the discussion, the above term is abbreviated by 'OUCP'.

The pressure of capillary water is determined by the ratio of curvature of the boundary between the capillary water and the air. The pressure of air surrounding the

Table 7 Velocities of Percolation at Equilibrium.

Soils / Intensity	Sandy soils S1	S2	L3	K	Loamy soils L1	L2	L3	L4
15mm/h*6h Sand 20mm/h* Loam 15mm/h*	(Equilibrium was not attained.)							
30mm/h*6h Sand 33mm/h* Loam 41mm/h*	F=31.4 W= 0.97 (16.1)	26.4 0.53 (8.8)	28.1 0.39 (6.5)	24.8 0.149 (2.5)	40.8 0.29 (4.9)	29.4 0.39 (6.4)	36.6 0.24 (4.0)	36.0 0.39 (6.6)
50mm/h*6h Sand 58mm/h* Loam 63mm/h*	F=58.0 W= 1.61 (27.)	58.0 0.98 (16.3)	36.3 0.61 (10.1)	55.3 [0.29] (4.8)	32.2 [0.39] (6.6)	52.0 [0.64] (11.0)	47.9 [0.32] (5.3)	52.0 [0.55] (9.1)

F(mm/h) : Intensity of discharge.
W(cm/min): Velocity in capillary, [ ] Evaluations by use of specific resistance, ( ) Conversion of W into (0.001cm/s).
* : Actual Intensity.

capillary is probably equal to that of the outside air. Actually, there are many types of curvature. If the materials of soil are uniform and the distribution of particle sizes are invariant at any part of the soil, the pressure of water inside the capillary may be constant everywhere because of the uniformity of distribution of the water curvature surrounding the capillary. Therefore, the pressure gradient in the capillary is considered to be 1, and the permeability of percolation is equal to the velocity of water in the capillary. The evaluated velocities (**W**) are shown in **Table 7**. These values are similar to the intensity of discharge (**F**) divided by the average increase of water volume at equilibrium against the water volume previous to the experiment for each soil. As the pressure gradient is 1, the velocity is equal to the permeability.
The relation used is,

$$\frac{r}{s} = v \stackrel{d}{=} K \tag{12}$$

where r (mm/s) is the intensity of discharge of the ground water, s is the average increase of water volume at equilibrium against the water volume previous to the experiment, v (mm/s) is the velocity, and K (mm/s) is the permeability.
Similar relation was investigated by Budagovskii (1955) and Rubin et. al. (1964). As this type of capillary was not formed before the experiment, the percolation at equilibrium might be realized in the capillary which was produced from the increased water. The increase in water volume was derived by use of data from the neuton scattering meter. Alternatively, the water content was evaluated by means of the theory of specific resistance, mentioned in the last chapter, for the assumption that the specific resistance of water was constant in the experiment.
In the case of **S1** (coarse sand) and **S2** (fine sand), under a rainfall of 30mm/h for 6h and 50mm/h for 6h, the permeability in **Table 7** corresponds to the velocity of the transmission front shown in **Table 5**. This is an additional evidence that percolation reached equilibrium after transit of the transmission front.

Result 5.

Specific resistance increased at all points in the soil soon after rainfall stopped. **Fig. 8ⓑ, 9ⓑ** and **Fig. 11ⓑ, 12ⓑ** show the increase of specific resistance after the rainfall ended.
Discussion.

Fig. 13, 14, 15 and **Fig. 16, 17, 18** show the specific resistance for **S1** (coarse sand), **S2** (fine sand) and **K** (Kanuma pumice) respectively, under the rainfall intensities of 30mm/h for 2h and 100mm/h for 2h respectively. Specific resistance began to increase after rainfall had stopped from the upper part of the ground to the lower part with time. The velocity of propagation of the increase became fast with increase of the intensity of discharge at equilibrium. The capillary rise in the period of rainfall became high with increase of the rainfall intensity, and the decrease of water content in the capillary was probably observed as the increase of specific resistance.

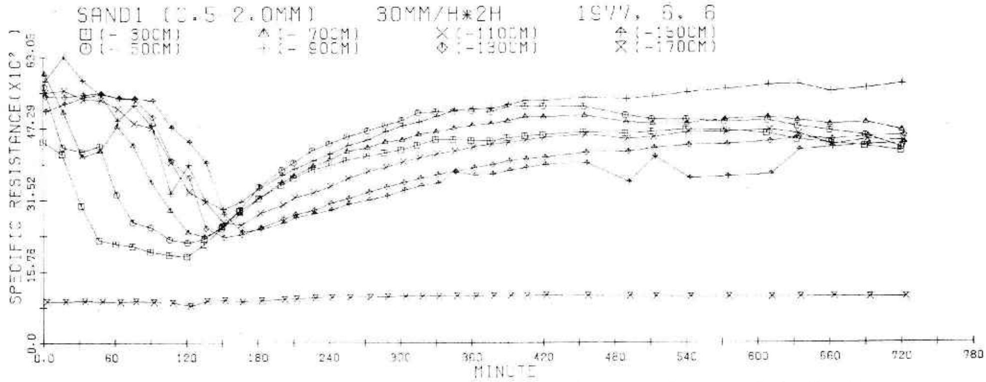

Fig. 13 Specific resistance curves showing time-varying vertical distribution of water content in Coarse Sand (S1), under a condition of rainfall of 30mm/h for 2 hours.

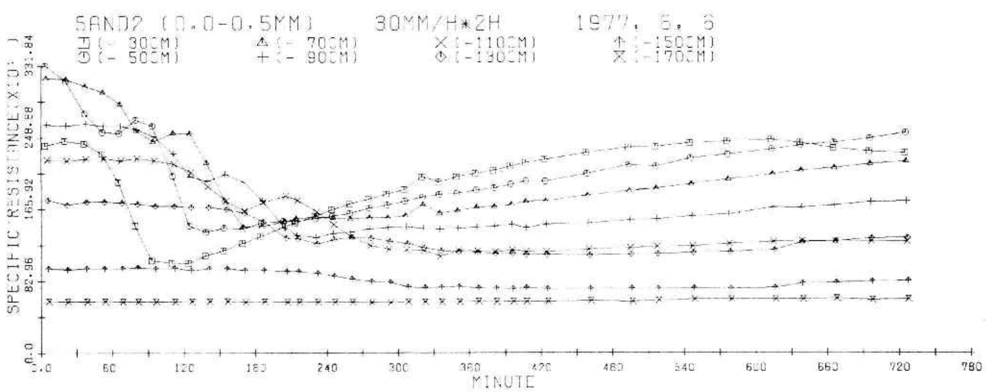

Fig. 14 Specific resistance curves for Fine Sand (S2), 30mm/h for 2 hours.

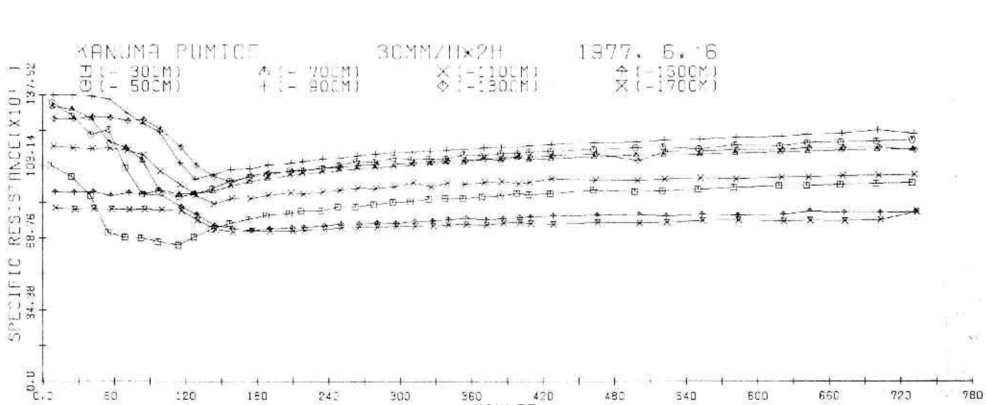

Fig. 15 Specific resistance curves for Kanuma Pumice (K), 30mm/h for 2 hours.

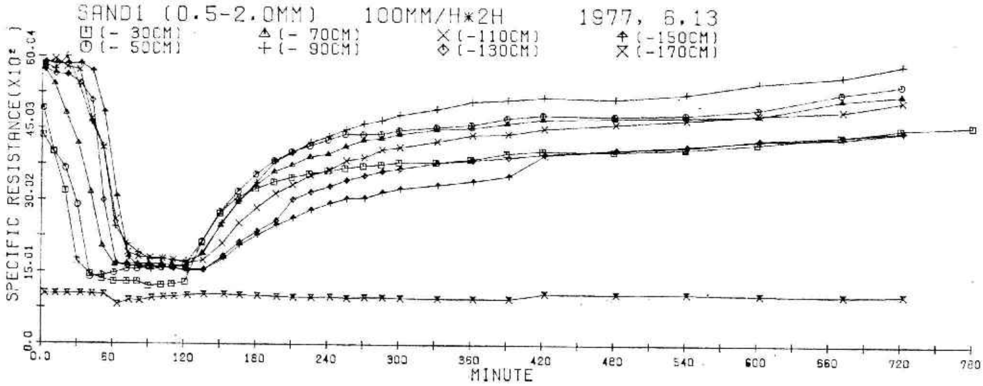

Fig. 16 Specific resistance curves showing time-varying vertical distribution of water content in Coarse Sand (S1), under a condition of rainfall of 100mm/h for 2 hours.

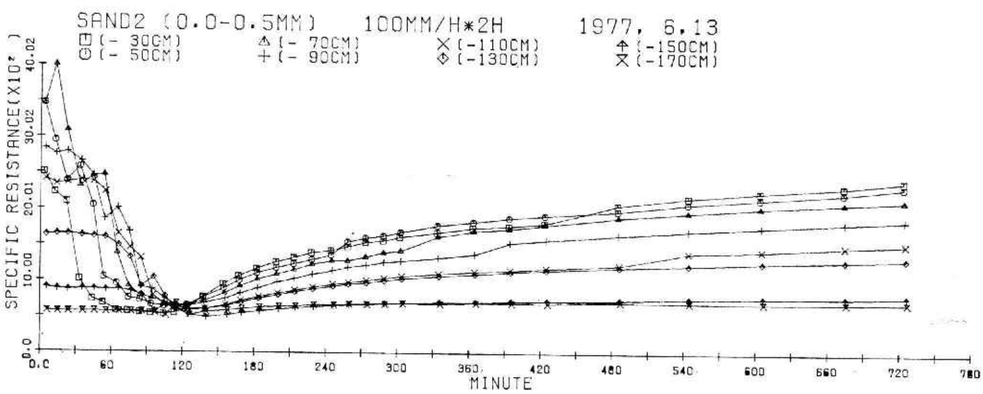

Fig. 17 Specific resistance curves for Fine Sand (S2), 100mm/h for 2 hours.

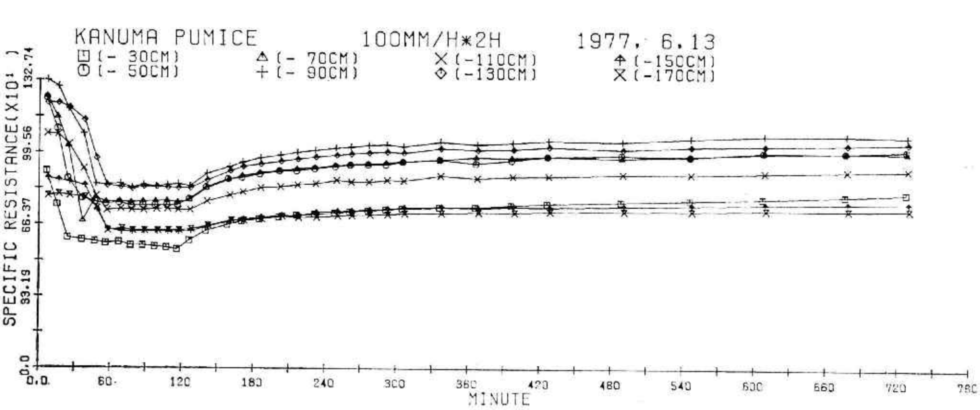

Fig. 18 Specific resistance curves for Kanuma Pumice (K), 100mm/h for 2 hours.

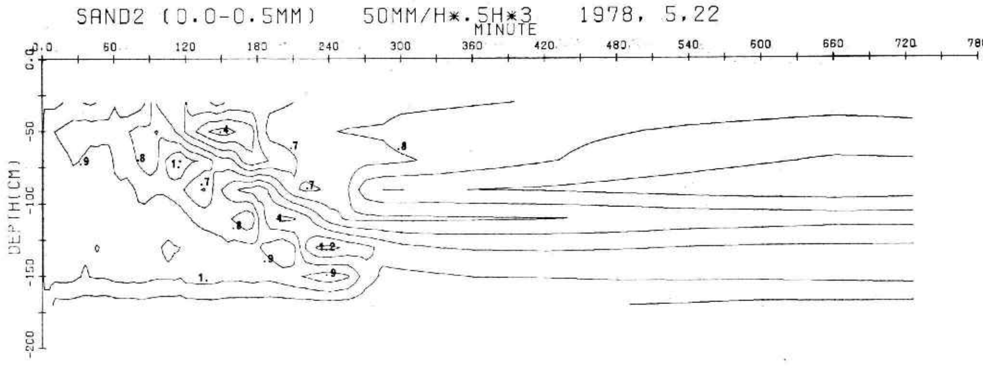

ⓐ Contour Map of Normalized Specific Resistance (see section 4-(4)).

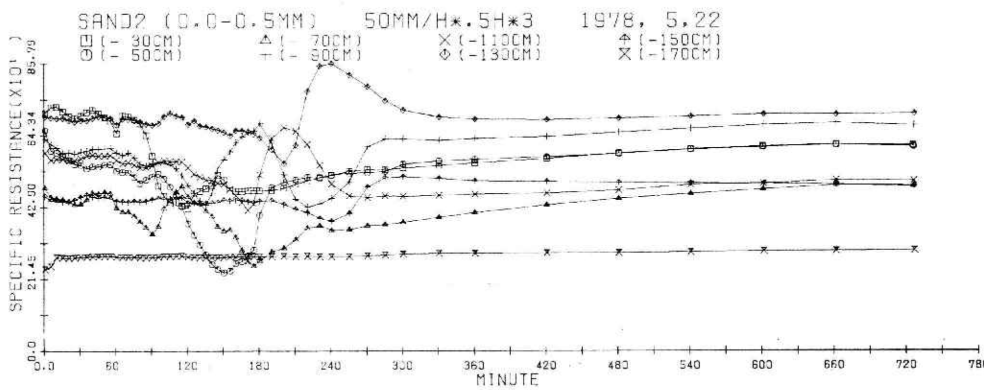

ⓑ Specific resistance curves showing time-varying vertical distribution of water content.

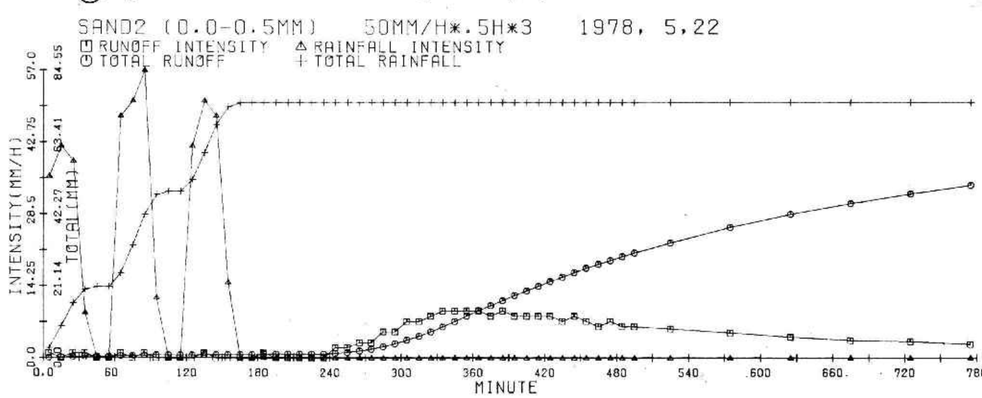

ⓒ Intensity of Rainfall and Discharge of Ground Water.

Fig. 19 Fine Sand (S2), 50mm/h for 0.5 hour for 3 times.

B. Alternating rectangular-type rainfall.

Fig. 19 shows the result of **S2** (fine sand) under a rainfall intensity of 50mm/h for 30 min for three times at an interval of 30min.

Result 6.

The decrease of specific resistance propagated from the surface to the inner part of the ground with time. It is recognized that specific resistance increased in periods of no rainfall. This is caused by movement of the low water content zone. This movement affected the intensity of the discharge.

(2) Results for loamy soils (L1, L2, L3, L4)

It is not easy to discriminate the transmission front in loamy soils as compared with sandy soils. Specific resistance decreases gradually in loamy soils with transit of the transmission front, though it changes rapidly in sandy soils. As velocities of the transmission front were similar in both soils, the thickness of the wetting zone, defined in **Fig. 5**, should be thin in sandy soils and thick in loamy soils. The term 'transmission front' has the above meaning in the present section.

A. Step-type rainfall.

Fig. 20, 21, 22 and **Fig. 23, 24, 25** are the results of **L1** (humic loam) and **L2** (compacted loam) respectively. ⓑin each figure shows the time variation of specific resistance in the loamy soils.

Result 1'.

The velocity of the transmission front increased when rainfall became intense, as shown in **Table 5**, with the exception of 50mm/h for 6h (mention later). The time lag from the beginning of rainfall until the transmission front reached −20cm from the surface of the ground decreased with the increase of rainfall intensity, especially in **L4** (stratified loam). In other soils (**L1, L2, L3**), the time lag was long when the intensity of rainfall was 50mm/h for 6h.

Discussion.

These phenomena are explained by the effect of 'ponding' around the surface area of the ground. The 'ponding' under discussion means not only the water film on the surface but also the isolation of the in/out flow of air around the surface. As in the case of sandy soils (see Result 4.), the above phenomena are explained by the 'OUCP' type of infiltration in loamy soils too, especially around the surface area. When the intensity of rainfall is small, replacement between air and water around the wetting zone can be performed smoothly and the transmission front descends continuously, because air in soil is connected to the outside air. The results of 15, 30, 50mm/h for 6h in sandy soils and 15, 30mm/h for 6h in loany soils are in accordance with the above condition. In contrast with this, the 'ponding' is formed around the surface area of the ground when rainfall becomes intense. In this case, it is difficult for the air replaced

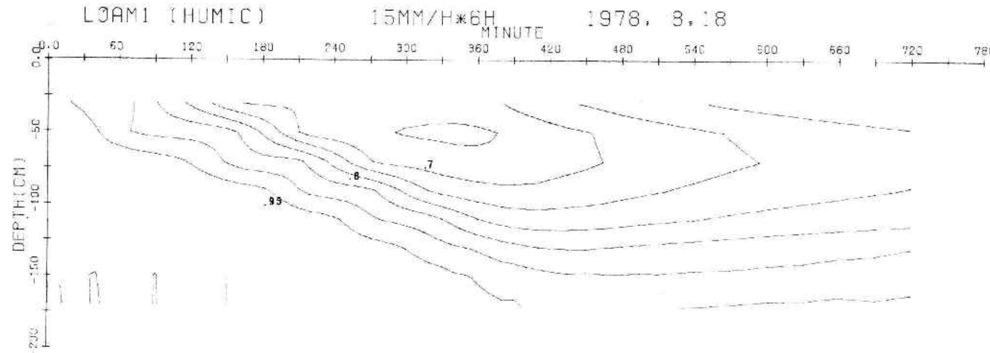

ⓐ Contour Map of Normalized Specific Resistance (see section 4-(4)).

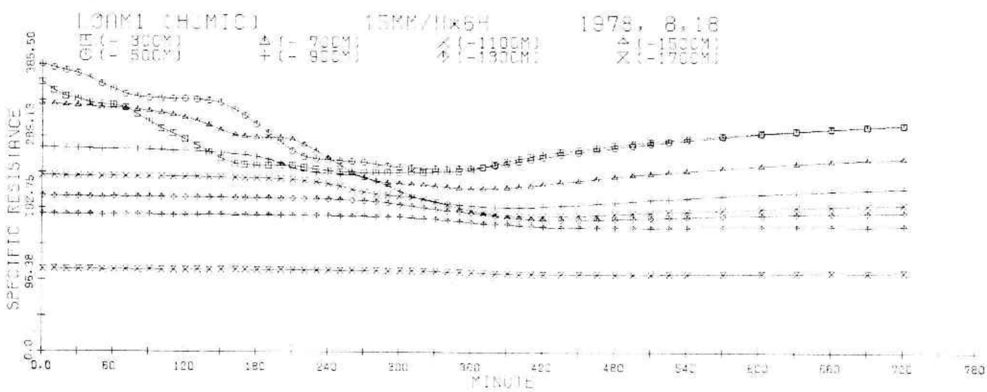

ⓑ Specific resistance curves showing time-varying vertical distribution of water content.

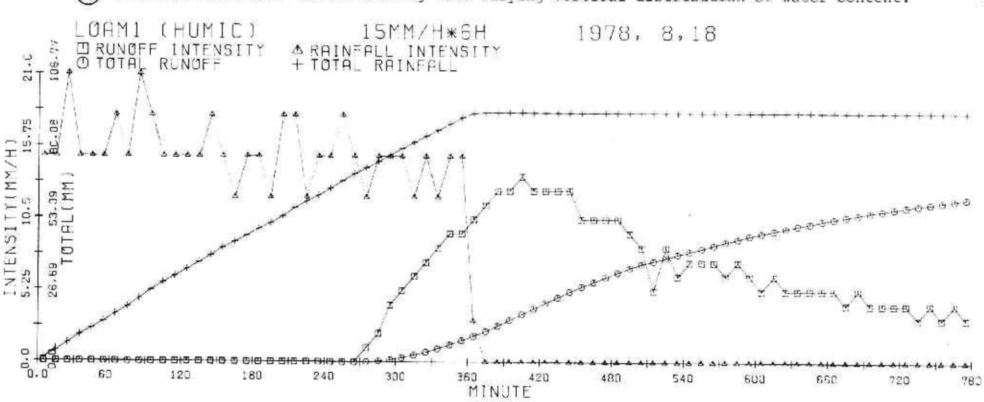

ⓒ Intensity of Rainfall and Discharge of Ground Water.

Fig. 20 Humic Loam (L1) 15mm/h for 6 hours

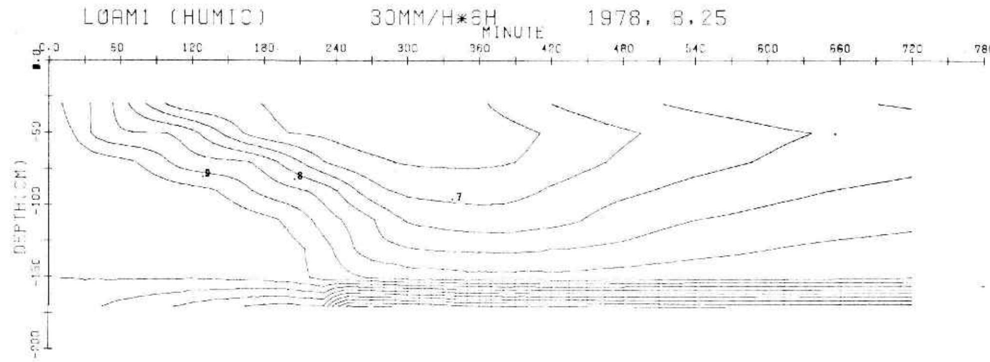

ⓐ Contour Map of Normalized Specific Resistance (see section 4-(4)).

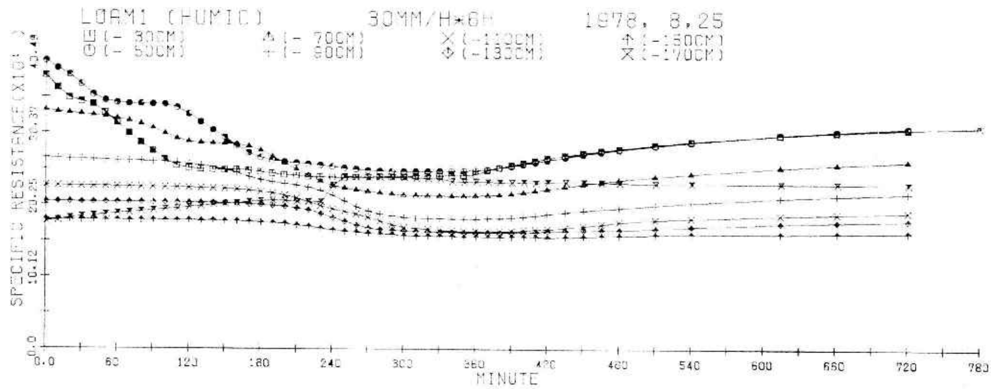

ⓑ Specific resistance curves showing time-varying vertical distribution of water content.

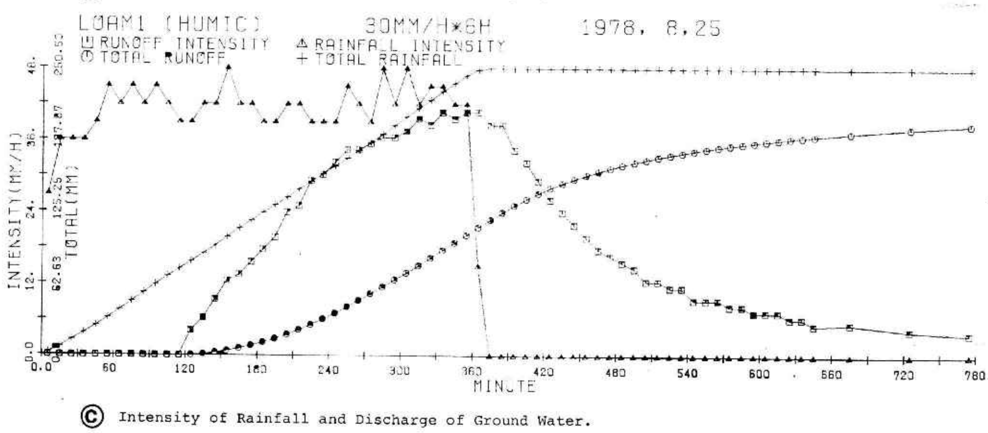

ⓒ Intensity of Rainfall and Discharge of Ground Water.

Fig. 21 Humic Loam (L1), 30mm/h for 6 hours.

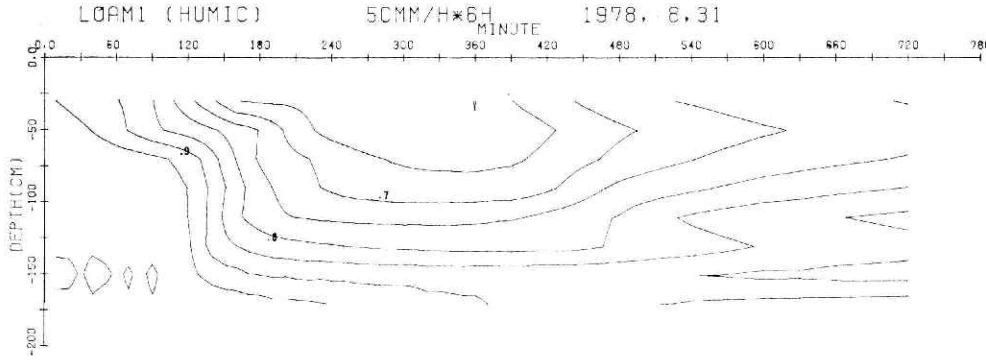

ⓐ Contour Map of Normalized Specific Resistance (see section 4-(4)).

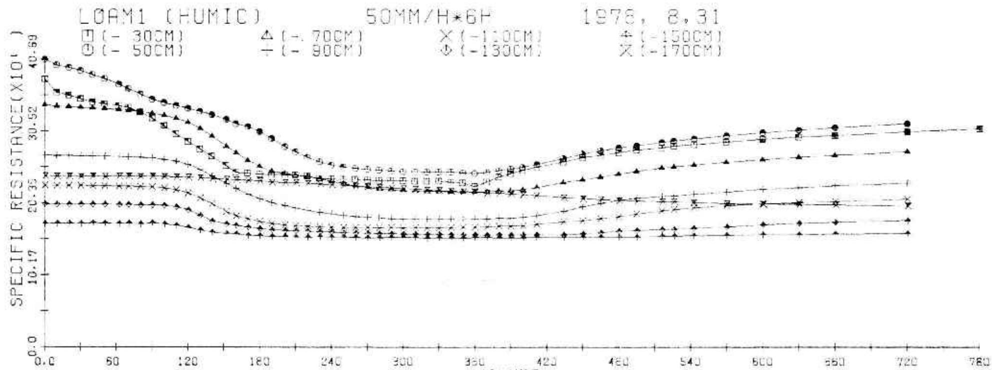

ⓑ Specific resistance curves showing time-varying vertical distribution of water content.

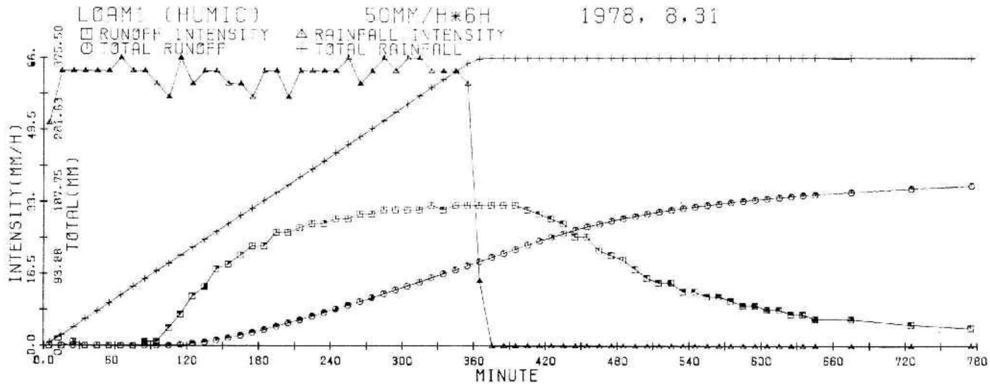

ⓒ Intensity of Rainfall and Discharge of Ground Water.

Fig. 22 Humic Loam (L1), 50mm/h for 6 hours.

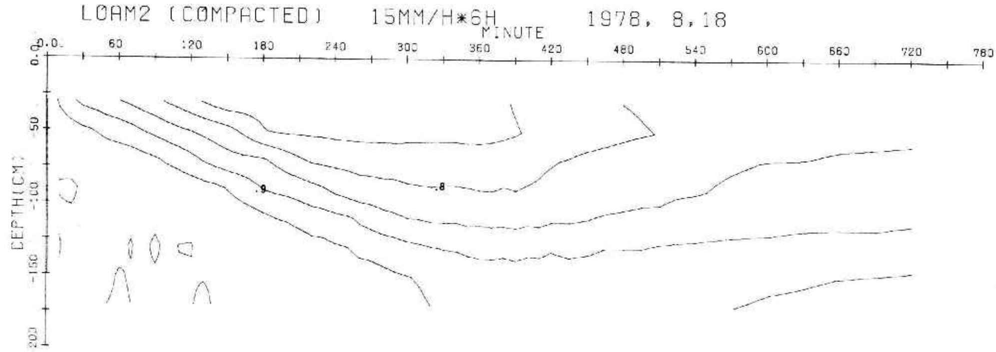

ⓐ Contour Map of Normalized Specific Resistance (see section 4-(4)).

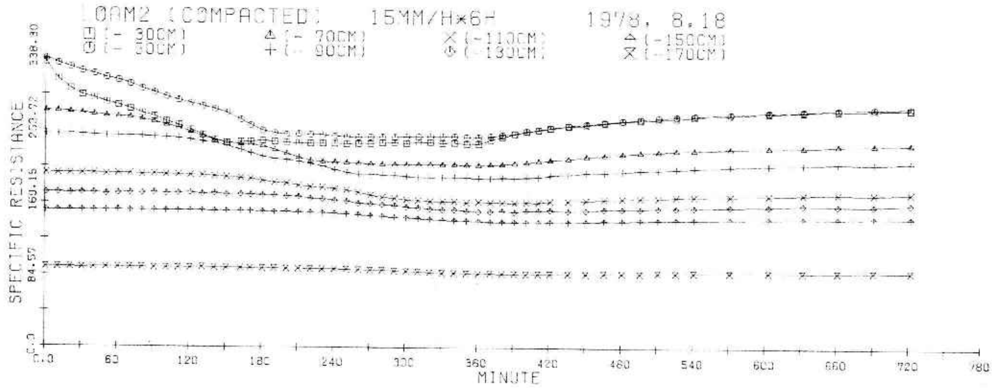

ⓑ Specific resistance curves showing time-varying vertical distribution of water content.

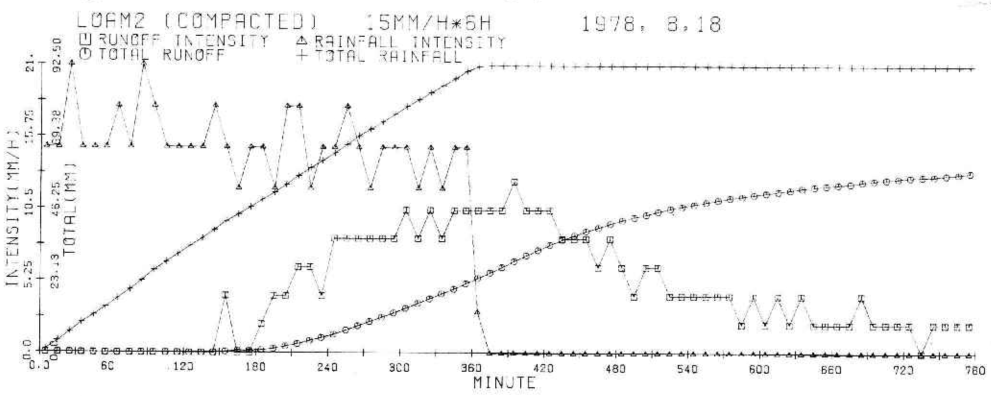

ⓒ Intensity of Rainfall and Discharge of Ground Water.

Fig. 23 Compacted Loam (L2), 15mm/h for 6 hours.

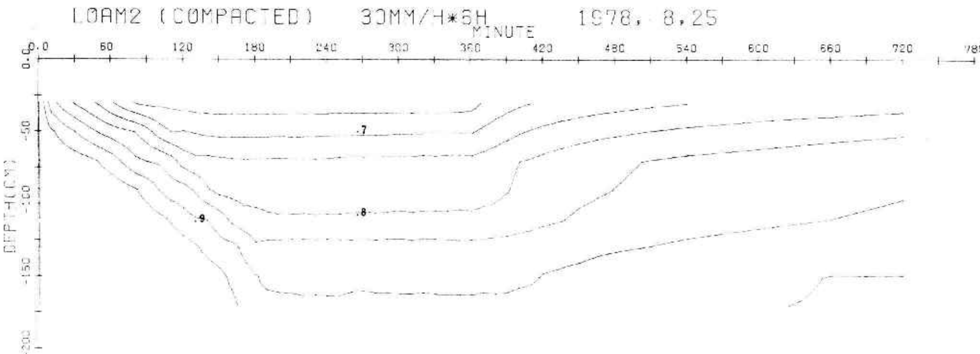

(a) Contour Map of Normalized Specific Resistance (see section 4-(4)).

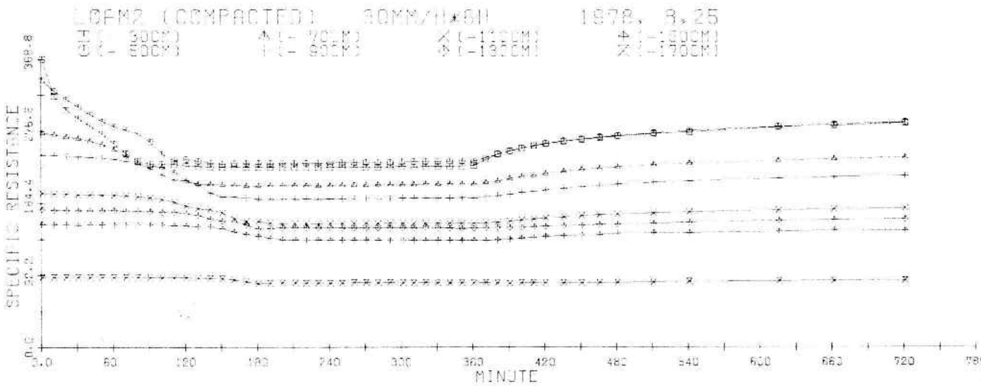

(b) Specific resistance curves showing time-varying vertical distribution of water content.

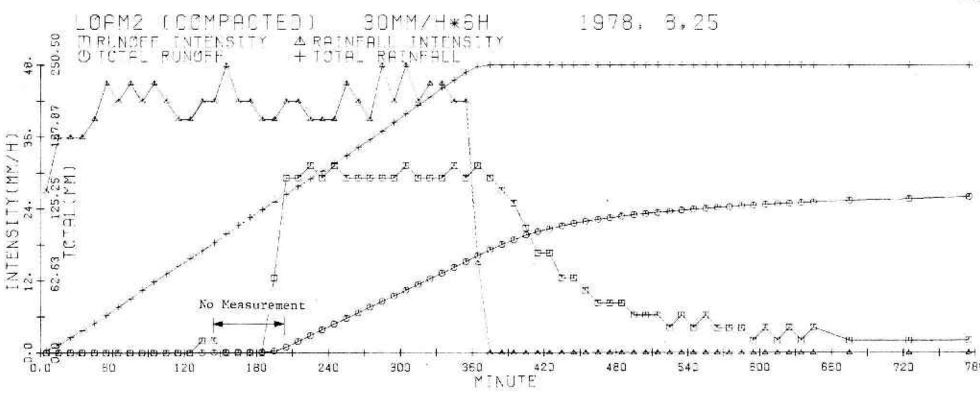

(c) Intensity of Rainfall and Discharge of Ground Water.

Fig. 24 Compacted Loam (L2), 30mm/h for 6 hours.

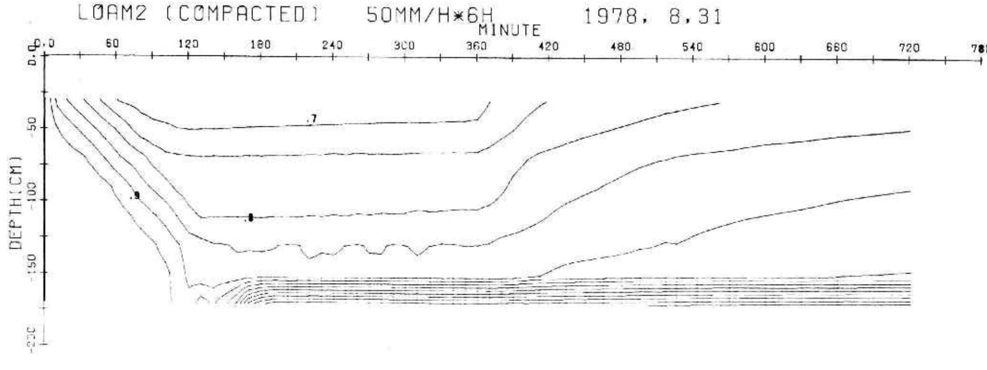

ⓐ Contour Map of Normalized Specific Resistance (see section 4-(4)).

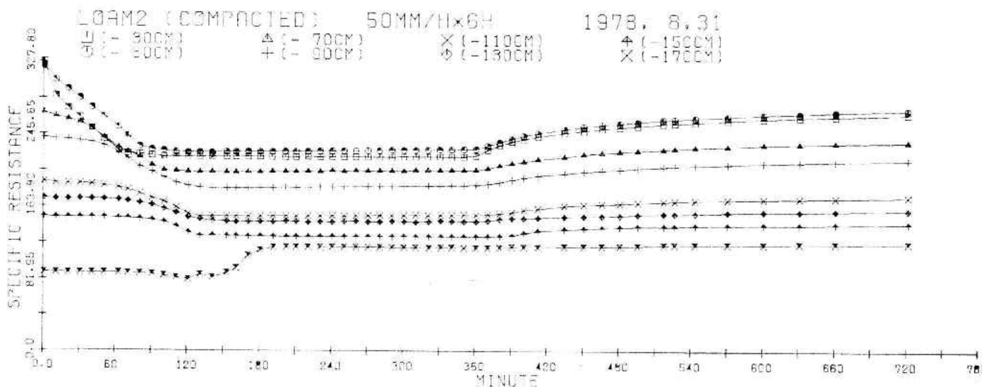

ⓑ Specific resistance curves showing time-varying vertical distribution of water content.

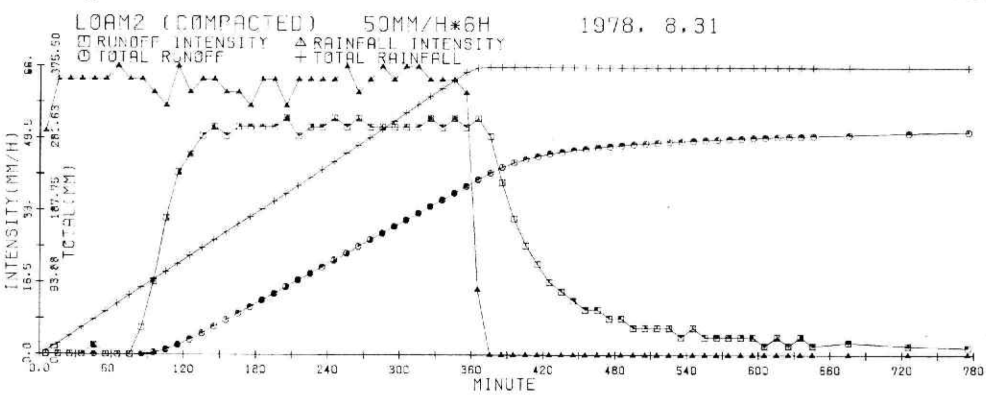

ⓒ Intensity of Rainfall and Discharge of Ground Water.

Fig. 25 Compacted Loam (L2), 50mm/h for 6 hours.

by water around the wetting zone to flow outside. As the terminal infiltration capacities of the experimental loams were about 35–45mm/h, the excess rainfall could not infiltrate the ground. This kind of water forms the 'ponding' around the surface area, and impedes the discharge of air to the outside. The air replaced by water around the wetting zone cannot move to the surface easily. Rainfall cannot infiltrate the ground, unless the capacity of air in the ground decreases. Therefore, it takes a long period for the transmission front to reach the −20cm point from the surface, and the accumulation of rainfall becomes large. Velocities of the transmission front around the surface area were small when the rainfall was 50mm/h for 6h in **L1** and **L4**, or the rate of increase of the velocity was small in **L2** and **L3**. These results can be attributed to the effect of temporary isolation of air around the surface area.

The velocity of the transmission front of **L2** (compacted loam), was faster than that of **L3** (uncompacted loam), for the forward movement force of the capillary in the wetting zone increased with the decrease of void size by compaction. The velocity of **L1** (humic loam) was smaller than that of **L2** and **L3**, because the humic zone was formed on the surface of the surface of the soil particles and resistance for water movement became large.

As the experiment continued, it became difficult to identify the transmission front especially in deep positions. This phenomenon was caused by the capillary rise which became high when total rainfall supplied to the ground model increased.

Result 2'.

Under constant and continuous rainfall, infiltration reached equilibrium with transit of the transmission front. After the transmission front reached the level of the ground water, the epuilibrium condition was observed at every depth in the soil.

Discussion.

As in the case of sandy soils, the specific resistance did not vary from some specific value after transit of the transmission front from the upper part to the lower part of the soil. **Fig. 20**ⓑ, **21**ⓑ, **22**ⓑ and **Fig. 23**ⓑ, **24**ⓑ, **25**ⓑ show this phenomenon. The inflow from upper part and the outflow to lower part were equal in this state, this condition was also mentioned in the case of sandy soils.

The capillary grew high in loamy soils as the experiments continued, so the transmission front disappeared around −70cm from the surface of the ground when the intensity of rainfall was 50mm/h. In such a case, the transmission front is supposed to have reached the level of the ground water when the specific resistance of the lower position became invariant. The transmission front reached the ground water level in the case of **Fig. 22**ⓐ after about 30min from the time when the transmission front disappeared at −60cm, and the intensity of the ground water discharge continued to be in equilibrium.

Result 3'.

The discharge of the ground water began before the transmission front reached the ground water level, shown in ⓐ and ⓑ of **Fig. 20, 21, 22** and **Fig. 23, 24, 25.**

Discussion.

There are two remarkable facts shown in **Table 6**, concerning namely, the time at which the discharge began (**U**), **a.** and the position of the transmissio front at that time (**H**), **b.**

a. The transmission front had not reached the level of the ground water when the discharge began.

b. The beginning time became early, and the position of the transmission front became high relative to the ground water level, when rainfall was intense.

Some models can be proposed to explain result **a.**

Model 1.

Water infiltrates through the cracks and voids developed in the soil.

Model 2.

The air, captured in the soil around the wetting zone. pushes water as a result of the pressure increase caused by the downward movement of infiltrating water.

Model 3.

The wetting front reaches the top of the capillary and water flows down through the capillary.

It is difficult to adopt Model 1, because the intensity of the ground water discharge did not continue at the same intensity, but gradually increased. If the water flowed through the crecks in the earlier stages, the intensity might continue at the same amount, and then might increase after the wetting front had reached the ground water. For Model 2, if air had moved downward and the soil-water content had decreased, possibly corresponding to the quantity of the discharge of ground water, the increase of the specific resistance must have been observed below the transmission front and above the ground water. This was not positively confirmed by the measurement of the specific resistance.

Model 3 is probable. In the capillary, the water content in the upper part is small but increases in the lower part. On the other hand, in the infiltrating water, the water content may be constant in the transmission zone and gradually decreases with depth in the wetting zone. Therefore, the discharge of the ground water begins around the time when the wetting front reaches the upper bound ot the capillary fringe and the discharge gradually becomes intense. The above mechanism explaines clearly the experimental results. Model 3 agrees with the fact that specific resistance began to decrease at any point below the transmission front when the discharge of the ground water began, although the height of the capillary could not be determined decisively.

Result **b** is attributed to the fact that the experiments were designed so that the intensity of rainfall increased as the experiments went on, which implies that the capillary grew high. The inclination of the curve of the normalized specific resistance representing the capillary rise became steep in **Fig. 20**ⓐ, **21**ⓐ, **22**ⓐ when the experiments continued. In addition to this phenomenon, the velocity of the wetting front increased following the result of **Table 5**, and the wetting front reached the upper bound of the capillary in a short period when the rainfall became intense. So, the beginning time of discharge became early. The water movement discussed in the present section is illustrated in Appendix.

The antecedent precipitation was often observed when the disasters occurred, such as landslide, slope failure, etc. According to the results mentioned above, the increase of the soil-water content by the antecedent precipitation, which also promotes the growth of the capillary rise, results in an early discharge of the ground water.

Result 4'.

Permeability of percolation at equilibrium was similar to the one of saturated infiltration in compasion with the one of unsaturated intiltration.

Discussion.

As in the case of sandy soils, percolation in loamy soils can be considered as the 'OUCP' type, when there is not 'ponding' around the surface of the ground (see Result 1'). The velocity of the transmission front is small when there is 'ponding'. The soil-water content around the surface area is small before rainfall begins, because water has evaporated since the last rainfall, so the velocity of the transmission front is expecially small in the area (see Result 1'). When the transmission front is descending, the air replaced by water in the wetting zone cannot be released freely to the outside by 'ponding' around the surface area, and this interferes with the air movement. In this case, air moves through the soil to the surface of the ground changing its shape, and that the shape of the boundary of the infiltrating water is not settled. After the disappearance of the transmission front into the ground water, replacement between water and air does not occur any more. So the volume of the air and water does not vary in the soil and the path of the percolation is settled. Therefore, after the equilibrium has been attained water percolates in the 'OUCP' manner, although there remains 'ponding' around the surface of the ground.

The pressure of air surrounding the capillary is not uniform. If the variation of pressure can be considered small, the pressure gradient in the capillary is almost equal to 1 as in the case of Result 4 for sandy soils. **Table 7** shows the velocity of percolation after the same procedure for sandy soils. In the case that the soil-water content was not measured by the neutron scattering meter, the water content was derived from other experiments by use of the theory mentioned in the section 4-(1) as in the case of sandy soils. The velocity of percolation (**W**) in **Table 7** was calculated on the assumption that the increase of the water volume widened the sectional area of the capillary, and percolating water went through this section. The value of **W** under discussion resembled the permeability of saturated infiltration which was derived from laboratory test.

Result 5'.

The increase of specific resistance began at the surface of the ground when rainfall stopped and it propagated to the lower part in the ground. The velocity of propagation was slower than that in sandy soils.

Discussion.

Fig. 20ⓑ, **21**ⓑ, **22**ⓑ and **Fig. 23**ⓑ, **24**ⓑ, **25**ⓑ show the rise in specific resistance after rainfall had stopped. Specific resistance increased slowly and it propagated from the upper part to the lower part of the ground. It is observed that the change propagated rapidly when the discharge of the ground water at equilibrium was intense.

B. Alternating rectangular-type rainfall.

Fig. 26 shows the results of **L2** (compacted loam) when the rainfall intensity was 50mm/h for 30min for three times at an interval of 30min.

Result 6'.

Fig. 26ⓒ shows that the pattern of intervals of ground water discharge corresponded to that of the rainfall pattern, although the pattern of the specific resistance could be recognized only at the point −30cm. The specific resistance did not change in the lower part.

Discussion.

The above phenomenon can be attributed to that the capillary had grown to a high level. The experiment which is shown in **Fig. 26** was the final experiment of the series. Before the experiment was conducted, seven types of rainfall had been supplied, with an interval of about a week. **Table 8** shows the time at which the discharge began, the accumulation of rainfall by thattime, the position of the tansmission front at that time evaluated by the velocity of the transmission front shown in **Table 5**, for the previous four experiments. The accumulation of rainfall and the position of the transmission front were almost equal in each experiment. Therefore, it is supposed that the rainfall had infiltrated the upper bound of the capillary fringe which had grown to the level of −45cm below the surface of the ground when the discharge of

Table 8 Several Variables of Experiments for Compacted Loam (L2).

Month/Day	Rainfall Input	Commencing Time of Discharge	R.I.*T	Location of Transmission Front
1978,	mm/h*h	min	mm	cm
9/ 6	50* 1	45	38	−45
9/12	100*.5	15	25	
9/18	30* 1 +70* 1	65	36	−50
9/25	50*.5 for 3 times	45	25	−45

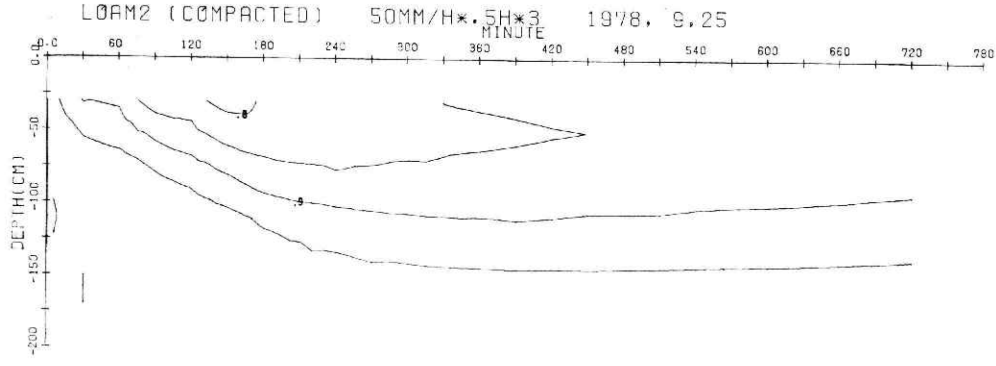

ⓐ Contour Map of Normalized Specific Resistance (see section 4-(4)).

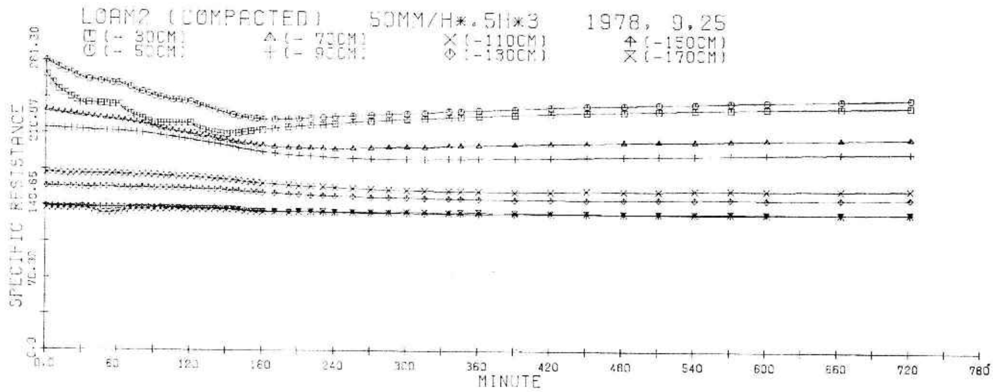

ⓑ Specific resistance curves showing time-varying vertical distribution of water content.

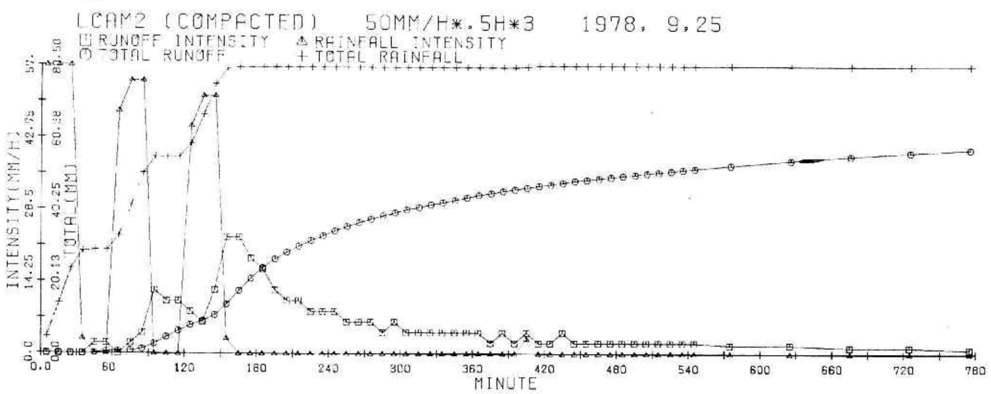

ⓒ Intensity of Rainfall and Discharge of Ground Water.

Fig. 26 Compacted Loam (L2), 50mm/h for 0.5 hour for 3 times.

the groud water began. The percolation which is one of the state of water movement (see **Fig. 5**) was realized in the capillary. Therefore, an increase of water volume and a dcrease of specific resistance were not observed. The result of **Fig. 26** is considered to be the profile view of the ground by the speific reristance which did not change.

6. Concluding remarks

The change of soil-water content in respone to rainfall was observed after a somewhat short period. Infiltrating water added additional water to the previously existing water in the soil. The velocity of infiltration was dependent on the intensity of rainfall, namely the velocity increased when the rainfall became intense. These results can be explained by the concept of the 'Open system-Unsaturated-Capillary-Percolation'. The period when there is no rainfall has an important role in the redistribution of the soil-water, in which water is redistributed in the soil and it is easy for the following rainfall, even if of low intensity, to infiltrate.

The rainfall pattern which is commonly used in the field of system dynamics has enabled some important facts, which might not be obtained using natural type of rainfall as input, to be revealed. The measurement must be chosen to fit the aim of the experiment. The specific resistance measurement agreed to some extent with the aim of the present experiments.

Acknowledgement

The writer wishes to express hearty thanks to Dr. Takeo Kinoshita, National Research Center for Disaster Prevention, for their worthwhile comments and discussions. The writer also wishes to express thanks to Professor Isamu Kayane and Mr. Ichiro Kaihotsu, Tsukuba University, for their contribution to the measurement of water content by means of the neutron scattering meter. Finally, the writer wishes to express thanks to Mr. Koki Tanaka and Mr. Hideo Aoki, for their operation of the rainfall simulator, and to the writer's colleagues for their mutual appreciation of the experiments.

Appendix

The changes of the degree of saturation and the total potential of soil-water from the beginning of rainfall infiltration until the discharge of the ground water begins are discussed in this section. Three kinds of heads are concerned with the movement of infiltrating water: elevation, pressure and total heads, which are indicated in the figures in this section by the capital E, P and T, respectively. These heads are connected by the following equation.

$$T = E + P$$

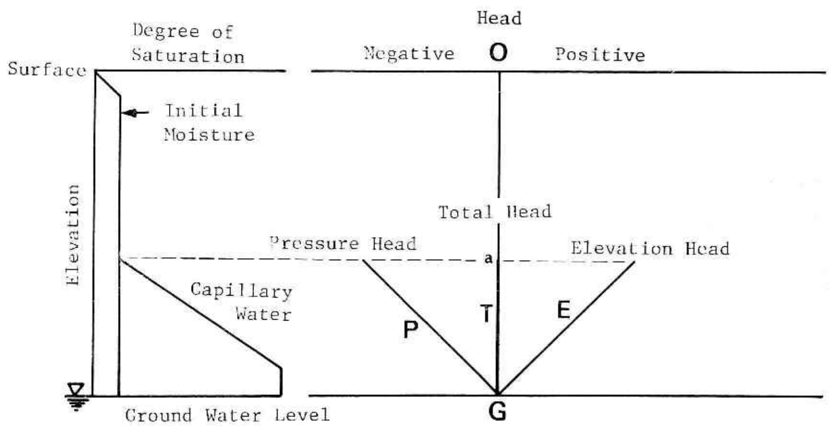

Fig. A1

Distribution of soil-water content before the rainfall is shown in **Fig. A1**. Pressure is propagated in the capillary water, but not in water above the capillary water. Water existing above the capillary before the rainfall is suspended among soil particles and is not moved by the gravity. Therefore, the water potential in this water can be excluded from the concerning total head. The total head in the capillary is uniform and the capillary water does not move.

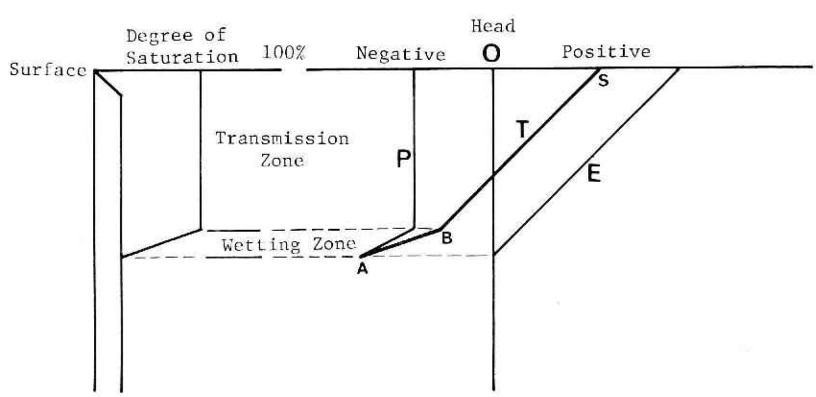

Fig. A2

Water content and heads of the infiltrating water are shown in **Fig. A2**. The water content becomes small with depth in the wetting zone, and the pressure head becomes small according to the degree of saturation. In the transmission zone, the water content is uniform and the pressure head is also uniform. (see Result 4 and 4') This phenomenon was investigated experimentally by Nakamura (1969),

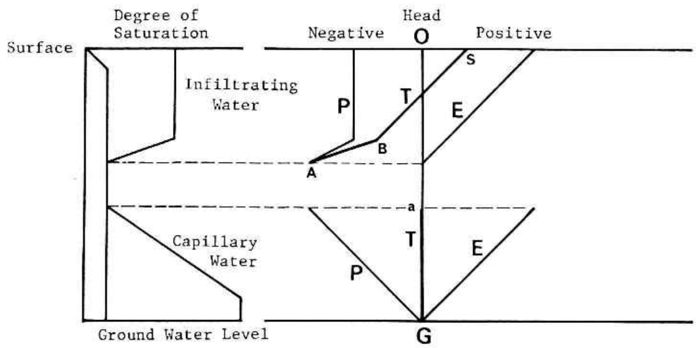

Fig. A3

The infiltrating and the capillary waters are shown in **Fig. A3** when rainfall continues. Both of waters are not connected hydraulically, so the origins of the elevation heads are not the same. The gradient of the total head is more steep in the wetting zone than in the transmission zone. On the other hand, the permeability in the wetting zone is smaller than in the transmission zone. Therefore, the amounts of the infintrating water for the same period of time in both zones are uniform under constant rainfall. (see Result 2 and 2')

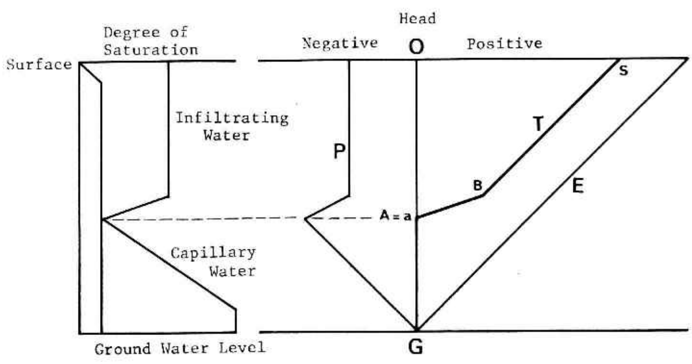

Fig. A4

The wetting front reaches the upper part of the capillary in **Fig. A4**, and the hydraulic continuity between both zones is realized. The elevation heads has the same origin for both waters.

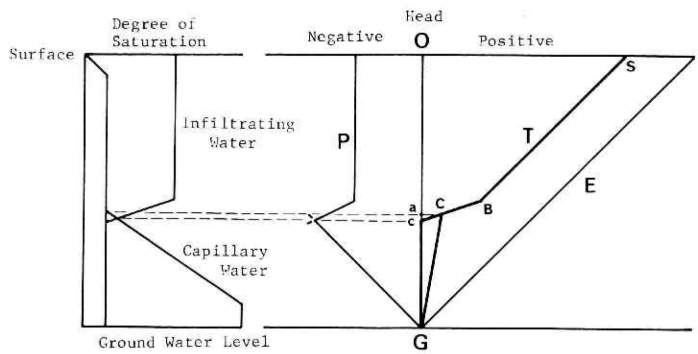

Fig. A5

In the connected zone of the infiltrating and the capillary water, the total head is within **c** and **C**. Then, the gradient of the total head in the capillary water varies from **cG** to **CG**, and makes the ground water flow.

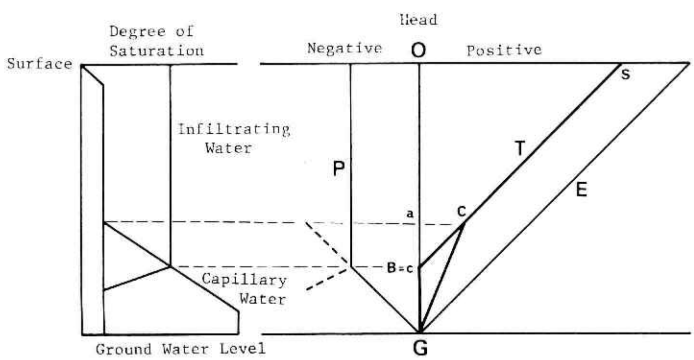

Fig. A6

The transmission front all reaches the capillary water. The gradient of the total head is within **cG** and **CG**. The increasing intensity of the ground water discharge is explained by the increase of the gradient of the total head and that of the sectional area of the capillary water in **Fig. A4**, **A5** and **A6**. (see Result 3 and 3')

References

1) Budagovskii, A. I. (1955): Infiltration of water into soil, USSR Academy of Sciences, Institute of Geography, Moscow. [Japanese translation by K. Muramoto, N. Nagata and T. Tabuchi. 1959.]

2) Hillel, D. (1971): Soil and Water, Academic Press.

3) Japanese Society of Soil Mechanics and Foundation Engineering. (1974): Earthwork Management and Radio Isotope, JSSMFE. [In Japanese.]

4) Katsurayama, K. (1957): Measurement of Soil-Water Content in Field by Electric Resistance Method, *Land Improvement*, Vol. **7**, No. 6, pp. 228–234. [In Japanese.]

5) MacDonald, A., Soled, J. and Stearns, C. (1953): Four-Probe Instrument for Resistivity Measurement of Germanium and Silicon, *Review of Scientific Instrument*, Vol. **24**, No. 9,

pp. 884-885.

6) Nakamura, T. (1969): Fundamental Researches on Percolation of Capillary Soil Water, *Memoirs of the College of Agriculture, Ehime University*, Vol. **14**, No. 1, pp. 1-106. [In Japanese.]

7) Rhoades, J. and Schilfgraarde, J. (1976): An electrical Conductivity Probe for Determining Soil Salinity, *Soil Science Society of America, Journal*, Vol. **40**, pp. 647-651.

8) Rubin, J., Steinhardt, R. and Reiniger, P. (1964): Soil Water Relations During Rain Infiltration: II. Moisture Content Profiles During Rains of Low Intensities, *Soil Science Society of America, Proceedings*, Vol. **28**, No. 1, pp. 1-5.

9) Takenaka, S. and Yamamoto, T. (1956): On the Determination of the Electric Resistivity by Wenner's Method with Specimens of Finite Dimensions, *Geophysical Exploration*, Vol. **9**, No. 3, pp. 101-104. [In Japanese.]

10) Tominaga, M. (1978): An Experiment of Infiltration in Large Scale Ground Models (1), *Report of the National Research Center for Disaster Prevention*, No. **20** pp. 123-135. [In Japanese.]

11) Tominaga, M. (1980): Experiments on Rain Infiltration in Soil (2) -Mathematical development of specific resistance of mixed materials for measurement of water content of soil-, *Report of the National Research Center for Disaster Prevention*, No. **23**, pp. 131-139.

12) Yamashita, A. (1971): Resistivity Studies of Sedimentary Strata, *Geophysical Exploration*, Vol. **24**, No. 3, pp. 14-23. [In Japanese.]

(Manuscript received December 18, 1979)

模擬地盤による降雨浸透実験（3）
―降雨浸透による地中水分変動と地下水流出―

富　永　雅　樹

国立防災科学技術センター国立防災科学技術センター大型降雨実験施設で行なった降雨浸透実験が述べられている．砂質土およびローム質土の土中水分が降雨入力に対応して示す変動を観察できるように実験が行なわれた．このため土の比抵抗測定法への考察を加え，それを実験で用いた．結果は次の様になった．

1．浸潤面（transmission zoneとwetting zone の境界部分）の下方への降下速度は，両土質ともに降雨強度が強くなるほど速くなる．

2．一定強度で持続する降雨の下では浸潤面の通過とともに浸透（percolation）は平衡状態になる．

3．地下水流出は浸潤前線（wetting front）が，地下水面上に発達した毛管水帯の上端に到達した時刻から始まる．

4．地下水流出強度を土中の体積含水率の増加分で割って求めた平衡状態での透水係数は室内試験で求めた飽和透水係数に近い値を示した．これは開放不飽和毛管浸透（浸透水は大気と連続している空気との気水界面をもつ毛管中を流れる）モデルによって説明される．

5．降雨中止後の比抵抗値の上昇は，土中の殆どあらゆる部分で短時間の間に発生した．

6．地表面付近の湛水（地表面上の水膜および土中水分の増加による土中と大気中の空気の切断によって土中の空気が自由に大気中へ開放されなくなることにより浸潤（infiltration）速度が遅くなる．